



Measurement of target spin (in)dependent asymmetries in dimuon production in pion-nucleon collisions at COMPASS



BAKUR PARSAMYAN

CERN, INFN section of Turin

on behalf of the COMPASS Collaboration

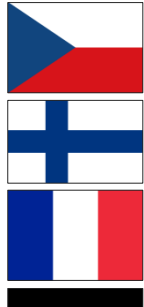


“XXIX International Workshop
on Deep Inelastic Scattering
and Related Subjects”

Santiago de Compostela, Spain
2-6 May 2022

COMPASS collaboration

Common Muon and Proton Apparatus for Structure and Spectroscopy



25 institutions from 13 countries
– nearly 200 physicists

- CERN SPS north area
- Fixed target experiment
- Approved in 1997
- Taking data since 2002

Wide physics program

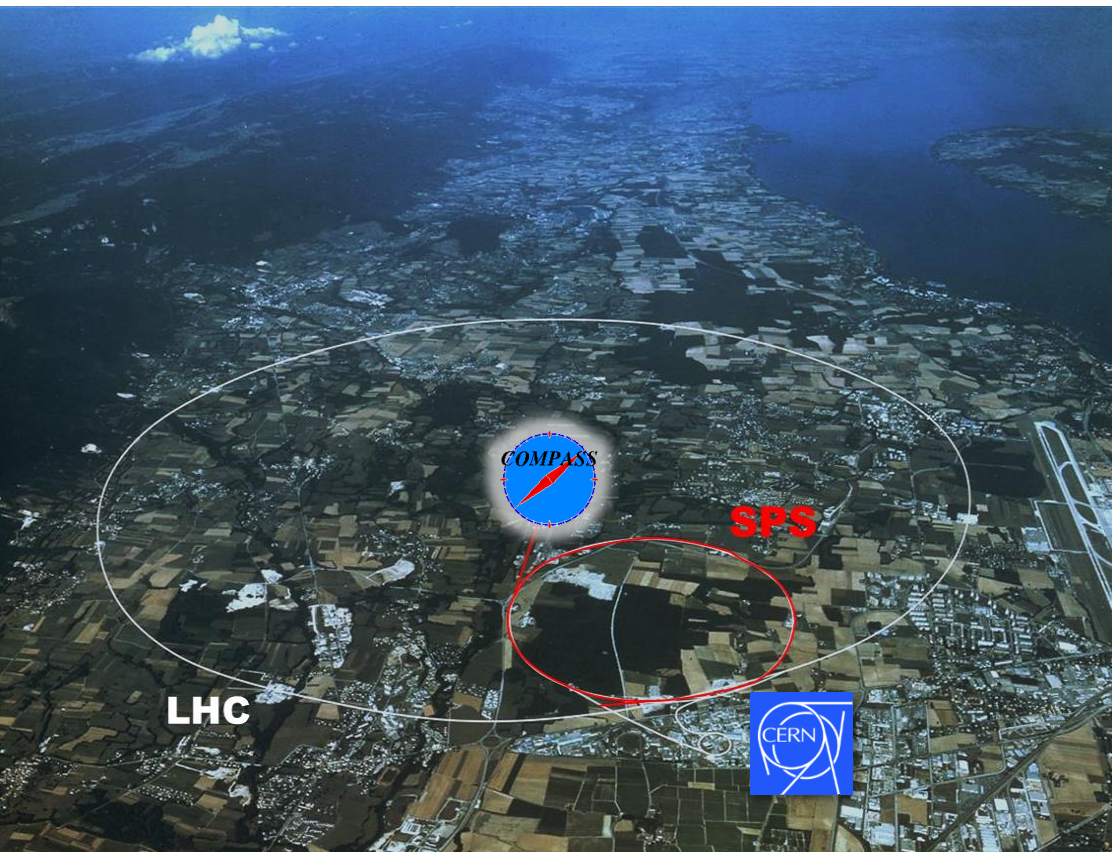
COMPASS-I

- Data taking 2002-2011
- Muon and hadron beams
- Nucleon spin structure
- Spectroscopy

COMPASS-II

- Data taking 2012-2022
- Primakoff
- DVCS (GPD+SIDIS)
- Polarized Drell-Yan
- Transverse deuteron SIDIS

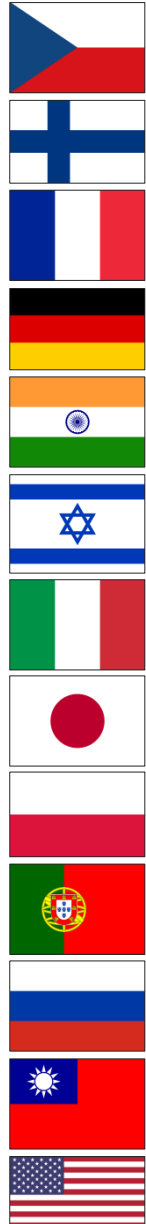
See also COMPASS talks by J.Giarra (DVCS) and J.Matousek (SIDIS)



COMPASS web page: <http://wwwcompass.cern.ch>

COMPASS collaboration

Common Muon and Proton Apparatus for Structure and Spectroscopy



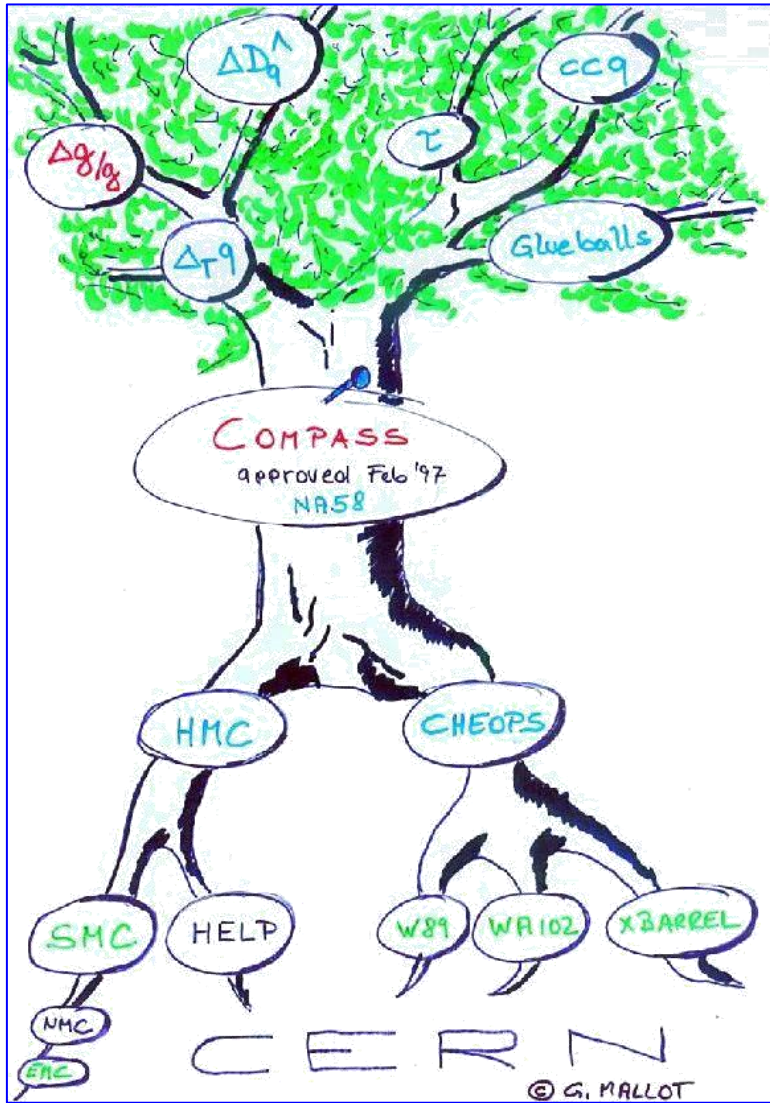
25 institutions from 13 countries
– nearly 200 physicists

- CERN SPS north area
- Fixed target experiment
- Approved in 1997 (**25 years**)
- Taking data since 2002 (**20 years**)

IWHSS-2022 workshop (**anniversary edition**)
CERN Globe, August 29-31, 2022



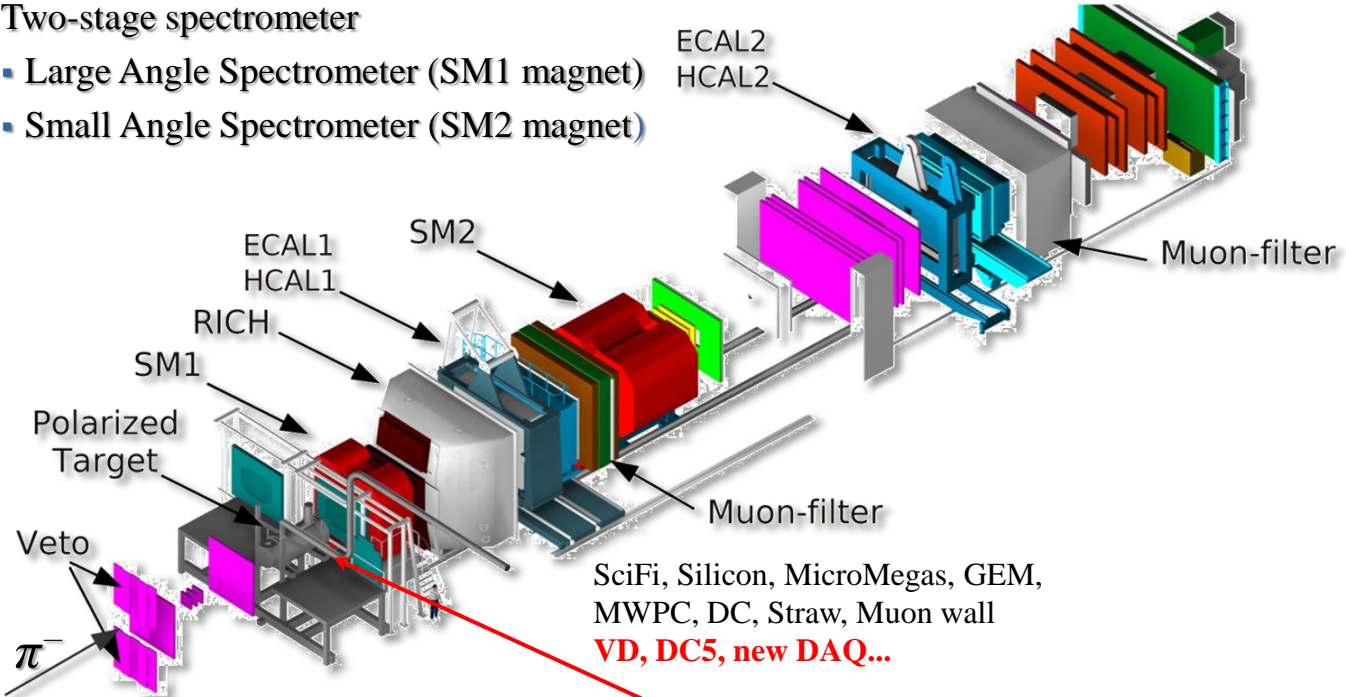
<https://indico.cern.ch/e/IWHSS-2022>



COMPASS experimental setup: Phase II (DY program)

Two-stage spectrometer

- Large Angle Spectrometer (SM1 magnet)
- Small Angle Spectrometer (SM2 magnet)



- High energy beam
- Large angular acceptance
- Broad kinematical range
- Momentum, tracking and calorimetric measurements, PID

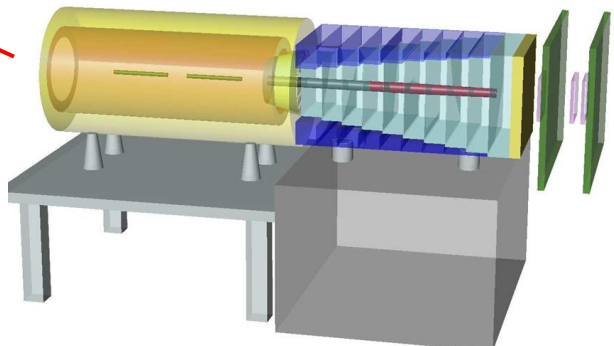
Data-taking years: 2014 (test) 2015 and 2018

High energy π^- beam:

Energy: 190 GeV/c, Intensity: $10^8 \pi/s$

Target: Solid state

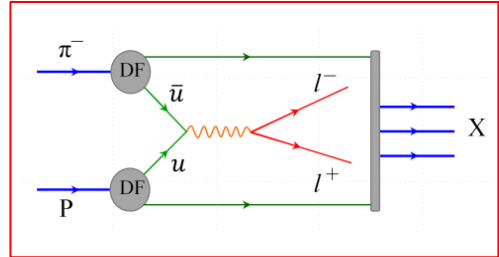
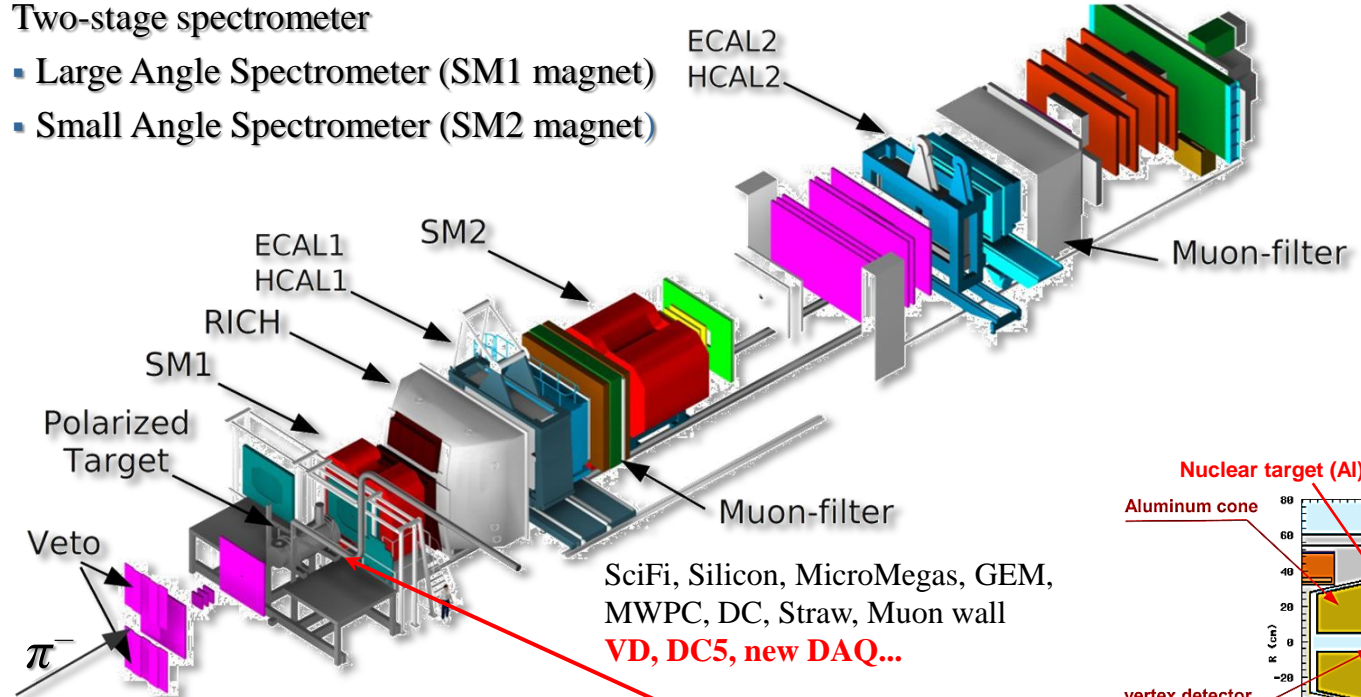
- NH_3 2-cell configuration. Polarization $T \sim 73\%$, $f \sim 0.18$



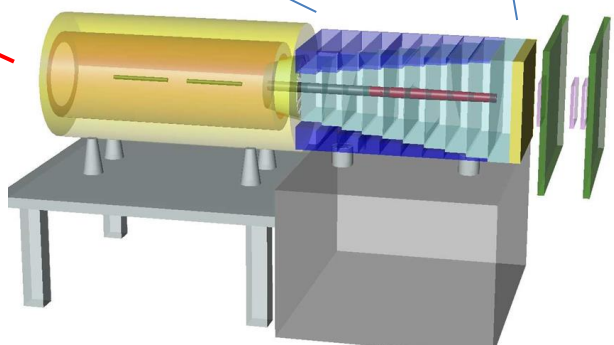
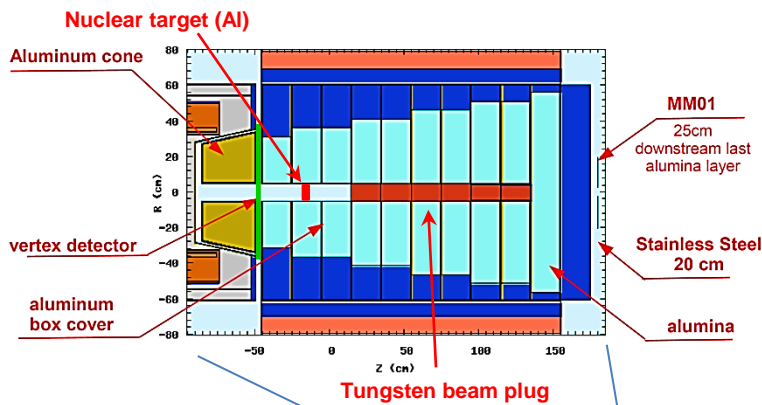
COMPASS experimental setup: Phase II (DY program)

Two-stage spectrometer

- Large Angle Spectrometer (SM1 magnet)
- Small Angle Spectrometer (SM2 magnet)



Hadron absorber



Data-taking years: 2014 (test) 2015 and 2018

High energy π^- beam:

Energy: 190 GeV/c, Intensity: $10^8 \pi/s$

Target: Solid state

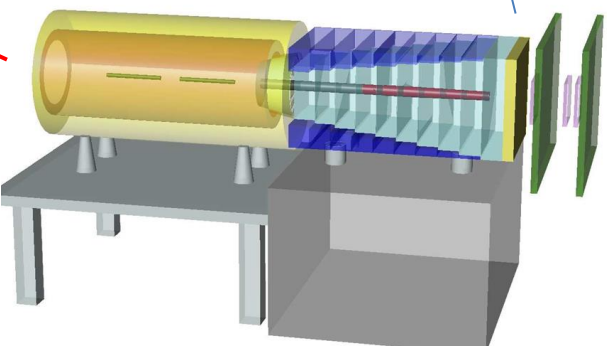
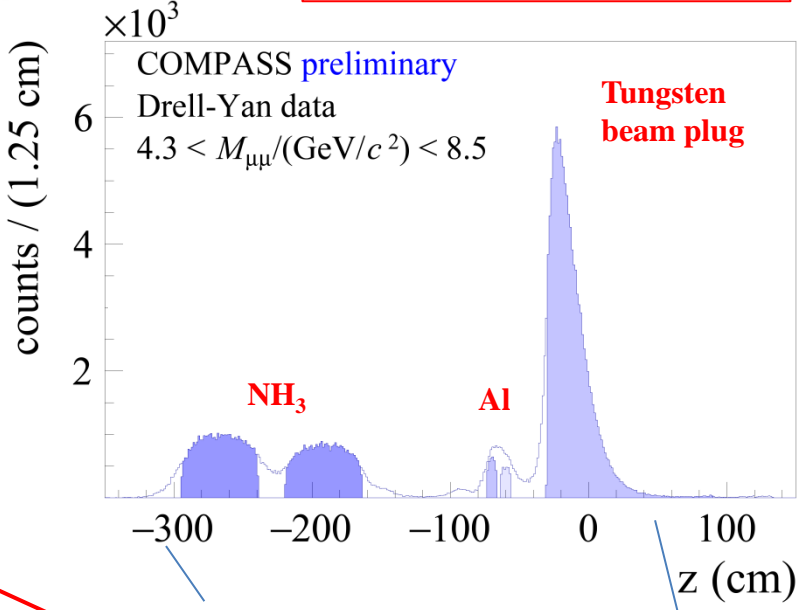
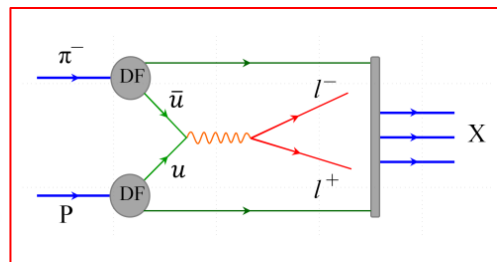
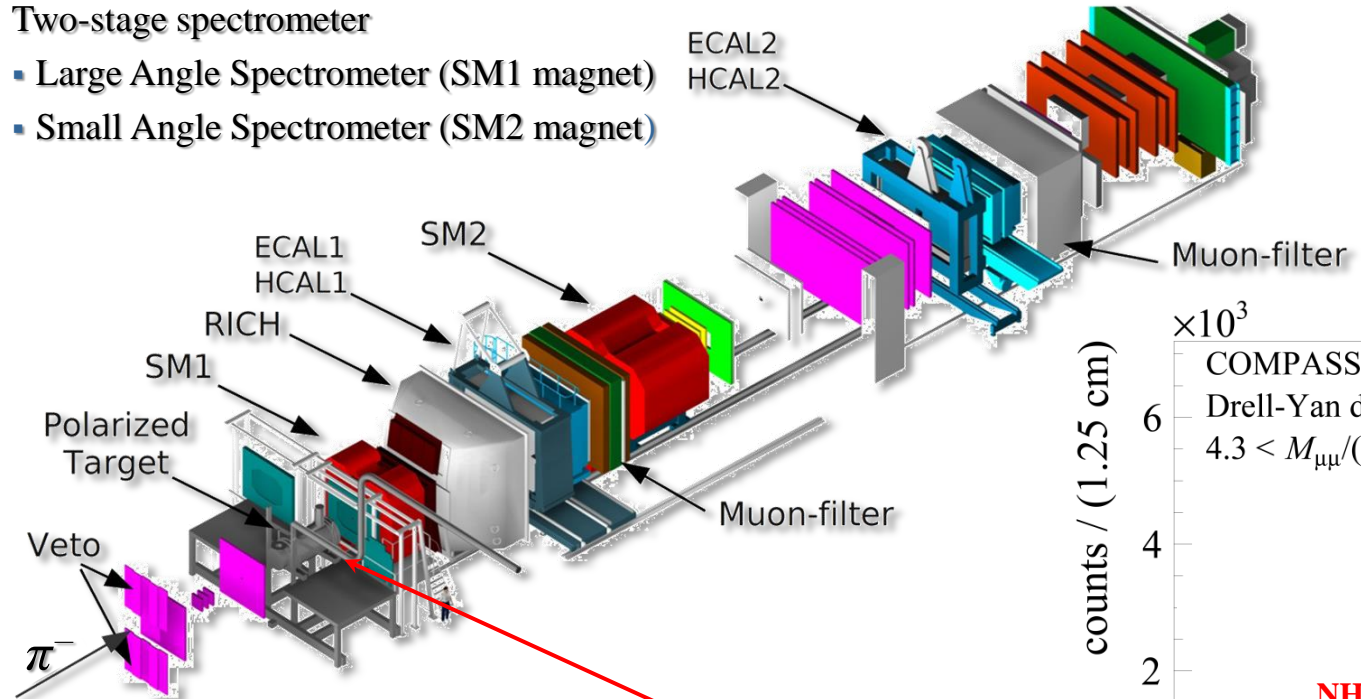
- NH₃ 2-cell configuration. Polarization T ~ 73%, f ~ 0.18

COMPASS experimental setup: Phase II (DY program)



Two-stage spectrometer

- Large Angle Spectrometer (SM1 magnet)
- Small Angle Spectrometer (SM2 magnet)



Data-taking years: 2014 (test) 2015 and 2018

High energy π^- beam:

Energy: 190 GeV/c, Intensity: $10^8 \pi/\text{s}$

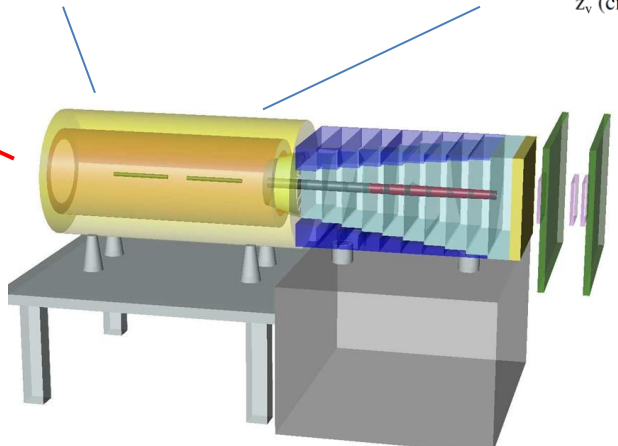
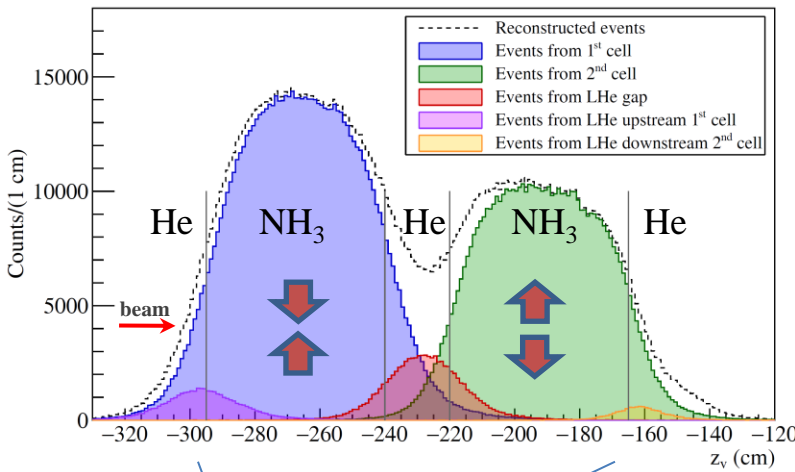
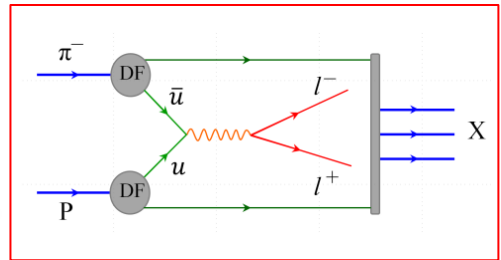
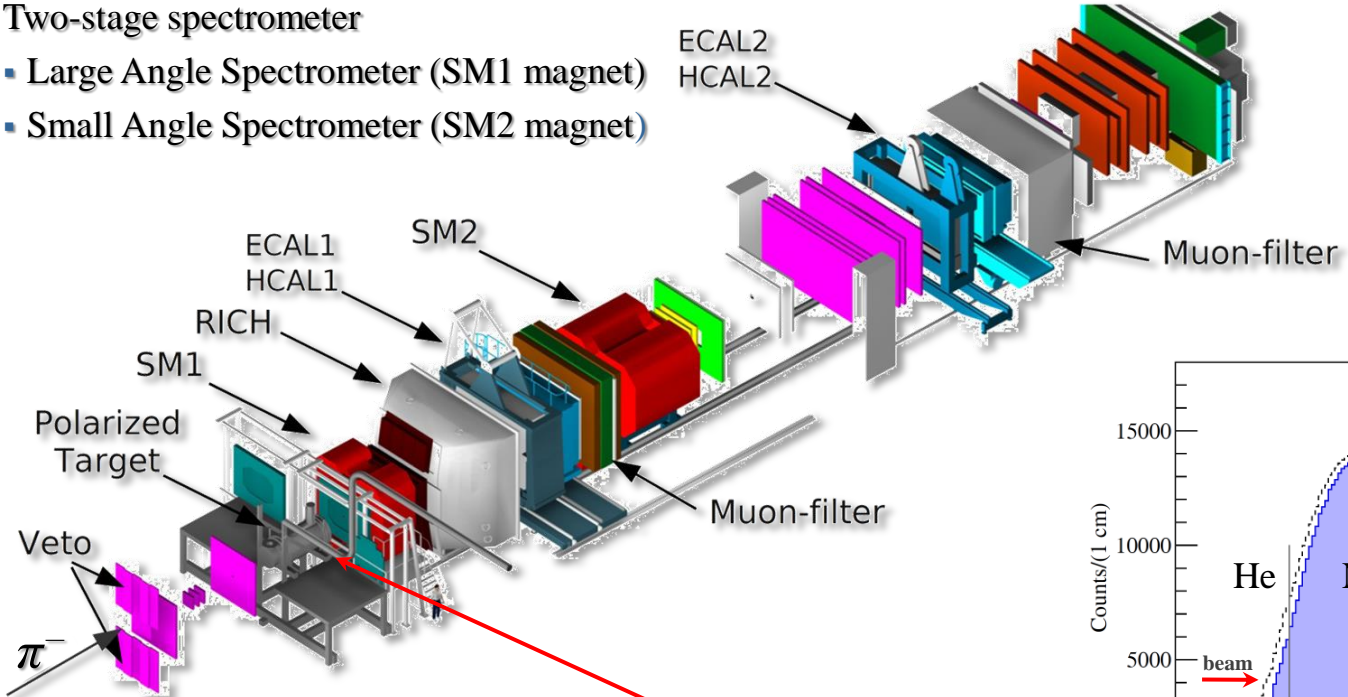
Target: Solid state

- NH_3 2-cell configuration. Polarization $T \sim 73\%$, $f \sim 0.18$

COMPASS experimental setup: Phase II (DY program)

Two-stage spectrometer

- Large Angle Spectrometer (SM1 magnet)
- Small Angle Spectrometer (SM2 magnet)



Data-taking years: 2014 (test) 2015 and 2018

High energy π^- beam:

Energy: 190 GeV/c, Intensity: $10^8 \pi/s$

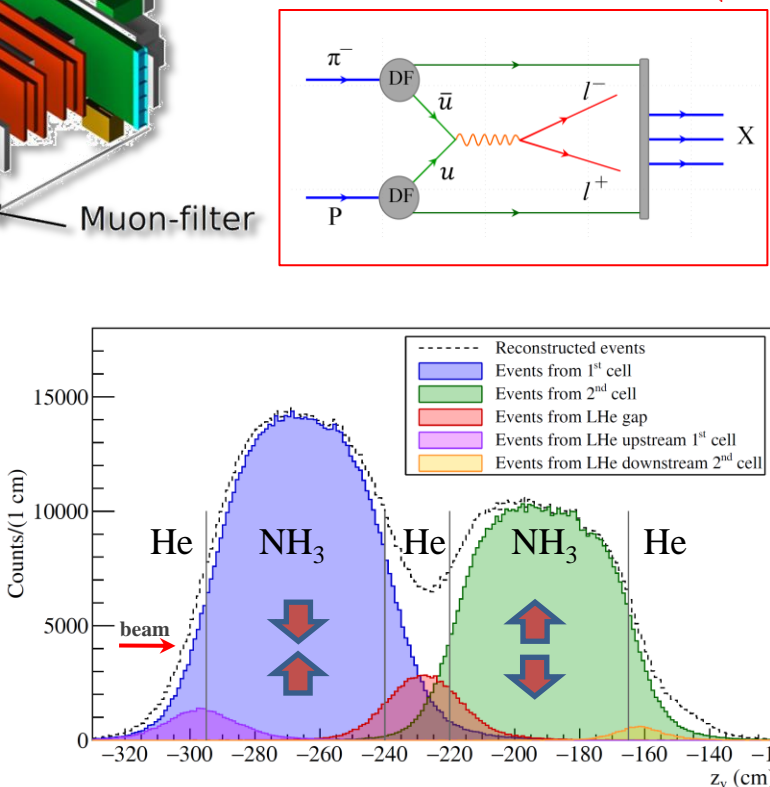
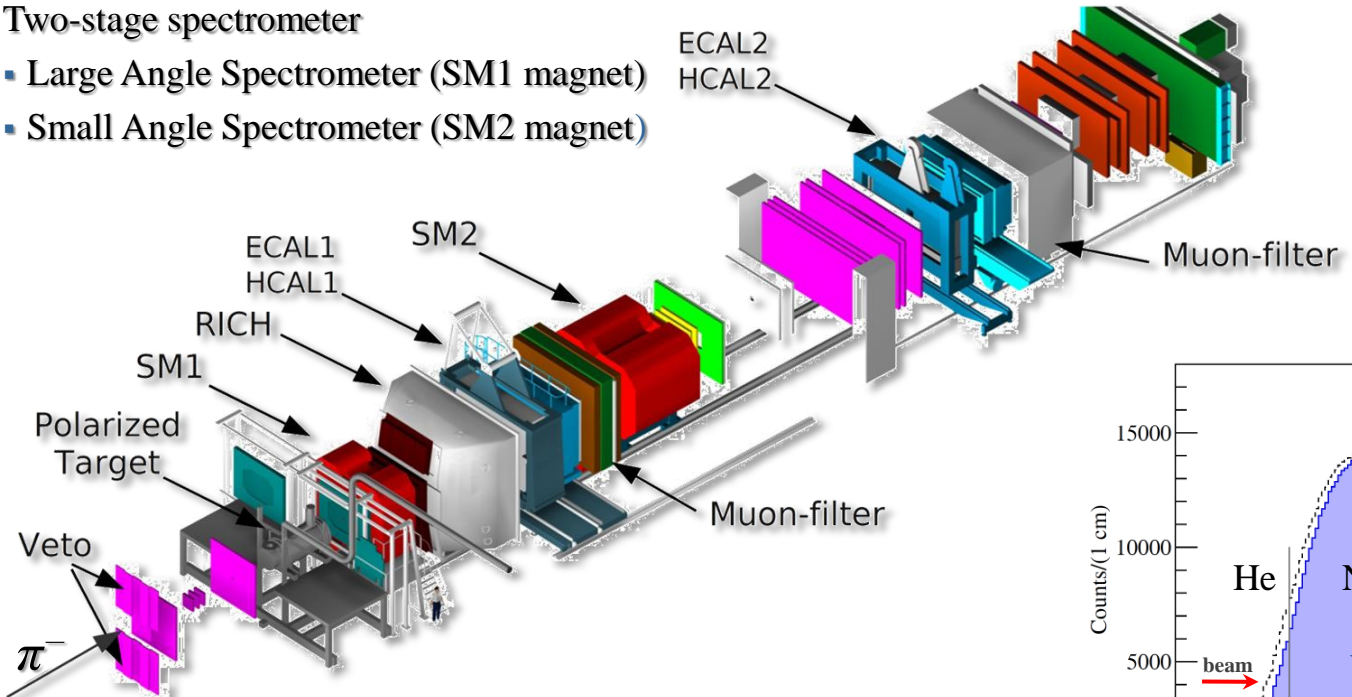
Target: Solid state

- NH_3 2-cell configuration. Polarization $T \sim 73\%$, $f \sim 0.18$
- Data is collected simultaneously with both target spin orientations
Periodic polarization reversal to minimize systematic effects

COMPASS experimental setup: Phase II (DY program)

Two-stage spectrometer

- Large Angle Spectrometer (SM1 magnet)
- Small Angle Spectrometer (SM2 magnet)



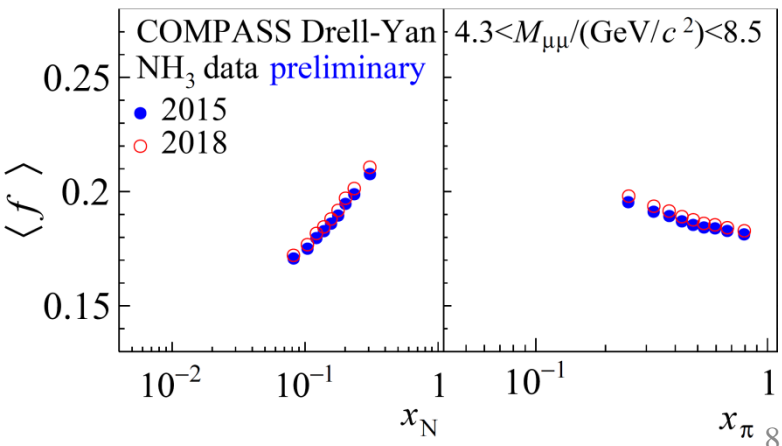
Data-taking years: 2014 (test) 2015 and 2018

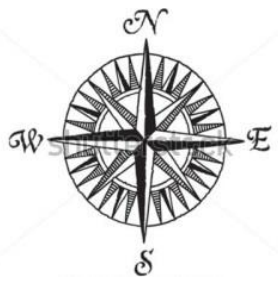
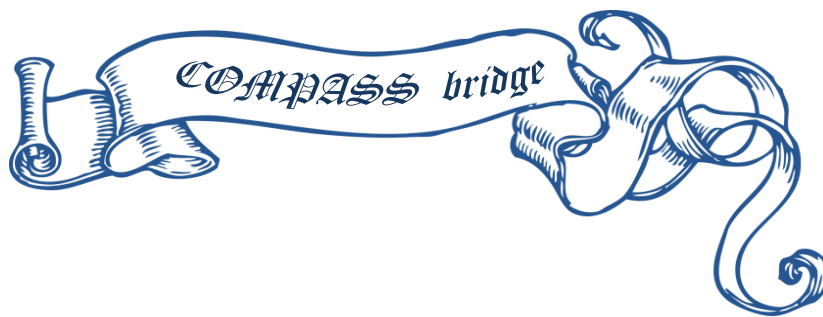
High energy π^- beam:

Energy: 190 GeV/c, Intensity: $10^8 \pi/s$

Target: Solid state

- NH_3 2-cell configuration. Polarization $T \sim 73\%$, $f \sim 0.18$
- Data is collected simultaneously with both target spin orientations
Periodic polarization reversal to minimize systematic effects





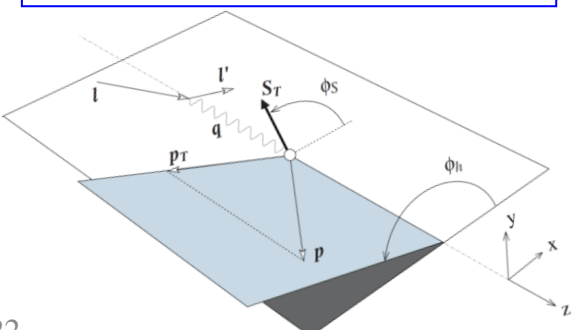
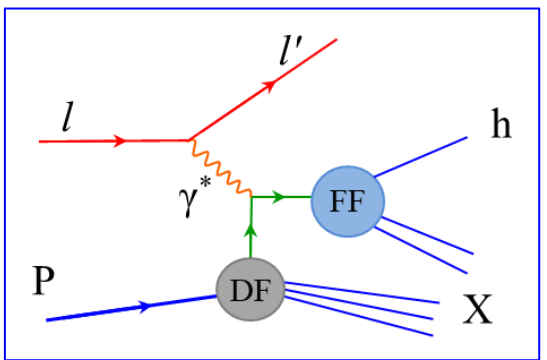
Drell-Pan

SIDS

SIDIS and single-polarized DY x-sections at twist-2 (LO)

$$\frac{d\sigma^{LO}}{dxdydzdp_T^2 d\phi_h d\phi_S} \propto (F_{UU,T} + \varepsilon F_{UU,L}) \quad \text{SIDIS}$$

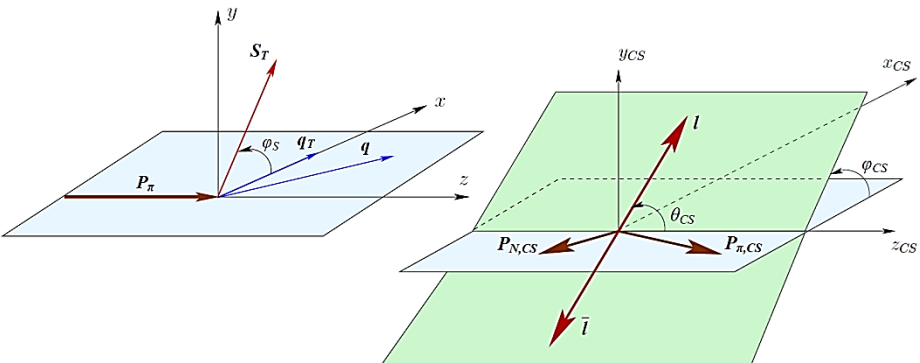
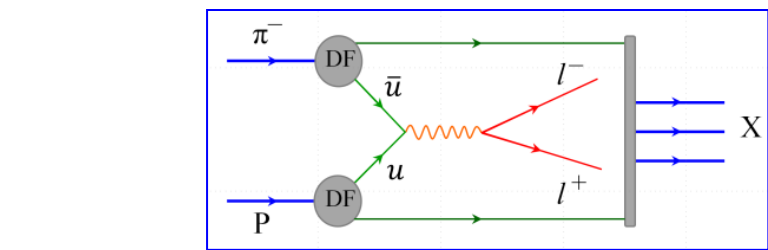
$$\times \left\{ \begin{array}{l} 1 + \boxed{\varepsilon A_{UU}^{\cos 2\phi_h} \cos 2\phi_h} \\ + S_L \varepsilon A_{UL}^{\sin 2\phi_h} \sin 2\phi_h + S_L \lambda \sqrt{1-\varepsilon^2} A_{LL} \\ \times \left[\begin{array}{l} A_{UT}^{\sin(\phi_h - \phi_S)} \sin(\phi_h - \phi_S) \\ + \varepsilon A_{UT}^{\sin(\phi_h + \phi_S)} \sin(\phi_h + \phi_S) \\ + \varepsilon A_{UT}^{\sin(3\phi_h - \phi_S)} \sin(3\phi_h - \phi_S) \end{array} \right] \\ + S_T \lambda \left[\sqrt{(1-\varepsilon^2)} A_{LT}^{\cos(\phi_h - \phi_S)} \cos(\phi_h - \phi_S) \right] \end{array} \right\}$$



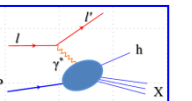
$$\frac{d\sigma^{LO}}{dq^4 d\Omega} \propto F_U^1 (1 + \cos^2 \theta_{CS}) \quad \text{DY}$$

$$\times \left\{ \begin{array}{l} 1 + \boxed{D_{[\sin^2 \theta_{CS}]} A_U^{\cos 2\phi_{CS}} \cos 2\phi_{CS}} \\ + S_L \sin^2 \theta_{CS} A_L^{\sin 2\phi_{CS}} \sin 2\phi_{CS} \\ \times \left[\begin{array}{l} A_T^{\sin \phi_S} \sin \phi_S \\ + D_{[\sin^2 \theta_{CS}]} \left(A_T^{\sin(2\phi_{CS} - \phi_S)} \sin(2\phi_{CS} - \phi_S) \right. \\ \left. + A_T^{\sin(2\phi_{CS} + \phi_S)} \sin(2\phi_{CS} + \phi_S) \right) \end{array} \right] \end{array} \right\}$$

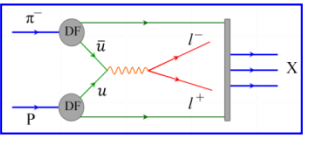
where $D_{[\sin^2 \theta_{CS}]} = \sin^2 \theta_{CS} / (1 + \cos^2 \theta_{CS})$



SIDIS and single-polarized DY x-sections at twist-2 (LO)

$$\frac{d\sigma^{LO}}{dx dy dz dp_T^2 d\phi_h d\phi_S} \propto (F_{UU,T} + \varepsilon F_{UU,L})$$


$$\times \left\{ \begin{array}{l} 1 + \boxed{\varepsilon A_{UU}^{\cos 2\phi_h} \cos 2\phi_h} \\ + S_L \varepsilon A_{UL}^{\sin 2\phi_h} \sin 2\phi_h + S_L \lambda \sqrt{1-\varepsilon^2} A_{LL} \\ \\ \times \left[\begin{array}{l} A_{UT}^{\sin(\phi_h - \phi_S)} \sin(\phi_h - \phi_S) \\ + \varepsilon A_{UT}^{\sin(\phi_h + \phi_S)} \sin(\phi_h + \phi_S) \\ + \varepsilon A_{UT}^{\sin(3\phi_h - \phi_S)} \sin(3\phi_h - \phi_S) \end{array} \right] \\ + S_T \lambda \left[\sqrt{(1-\varepsilon^2)} A_{LT}^{\cos(\phi_h - \phi_S)} \cos(\phi_h - \phi_S) \right] \end{array} \right\}$$

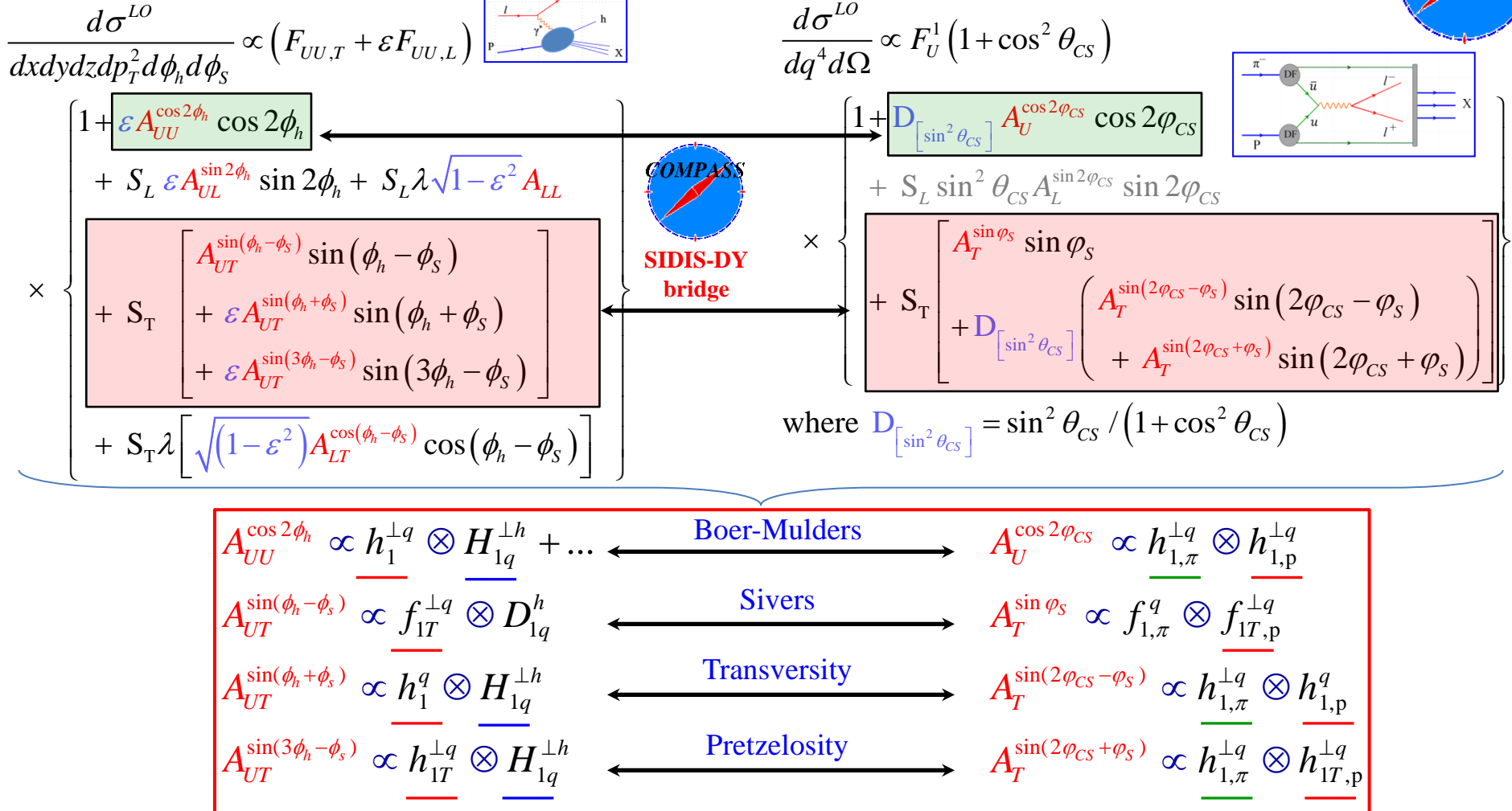
$$\frac{d\sigma^{LO}}{dq^4 d\Omega} \propto F_U^1 (1 + \cos^2 \theta_{CS})$$


$$\times \left\{ \begin{array}{l} 1 + \boxed{D_{[\sin^2 \theta_{CS}]} A_U^{\cos 2\phi_{CS}} \cos 2\phi_{CS}} \\ + S_L \sin^2 \theta_{CS} A_L^{\sin 2\phi_{CS}} \sin 2\phi_{CS} \\ \times \left[\begin{array}{l} A_T^{\sin \phi_S} \sin \phi_S \\ + D_{[\sin^2 \theta_{CS}]} \left(A_T^{\sin(2\phi_{CS} - \phi_S)} \sin(2\phi_{CS} - \phi_S) \right. \\ \left. + A_T^{\sin(2\phi_{CS} + \phi_S)} \sin(2\phi_{CS} + \phi_S) \right) \end{array} \right] \end{array} \right\}$$

where $D_{[\sin^2 \theta_{CS}]} = \sin^2 \theta_{CS} / (1 + \cos^2 \theta_{CS})$

Quark Nucleon	U	L	T
U	$f_1^q(x, \mathbf{k}_T^2)$ number density		$h_1^{\perp q}(x, \mathbf{k}_T^2)$ Boer-Mulders
L		$g_1^q(x, \mathbf{k}_T^2)$ helicity	$h_{1L}^{\perp q}(x, \mathbf{k}_T^2)$ worm-gear L
T	$f_{1T}^{\perp q}(x, \mathbf{k}_T^2)$ Sivers	$g_{1T}^q(x, \mathbf{k}_T^2)$ Kotzinian- Mulders worm-gear T	$h_1^q(x, \mathbf{k}_T^2)$ transversity $h_{1T}^{\perp q}(x, \mathbf{k}_T^2)$ pretzelosity

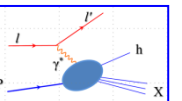
SIDIS and single-polarized DY x-sections at twist-2 (LO)



Complementary information from two different channels :

- SIDIS-DY bridging of nucleon TMD PDFs; Universality studies;
- Sign-change T-odd Sivers and Boer-Mulders TMD PDFs;
- Multiple access to Collins FF $H_{1q}^{\perp h}$ and pion Boer-Mulders PDF $h_{1,\pi}^{\perp q}$

SIDIS and single-polarized DY x-sections at twist-2 (LO)

$$\frac{d\sigma^{LO}}{dxdydzdp_T^2 d\phi_h d\phi_S} \propto (F_{UU,T} + \varepsilon F_{UU,L})$$


$$\frac{d\sigma^{LO}}{dq^4 d\Omega} \propto F_U^1 (1 + \cos^2 \theta_{CS})$$

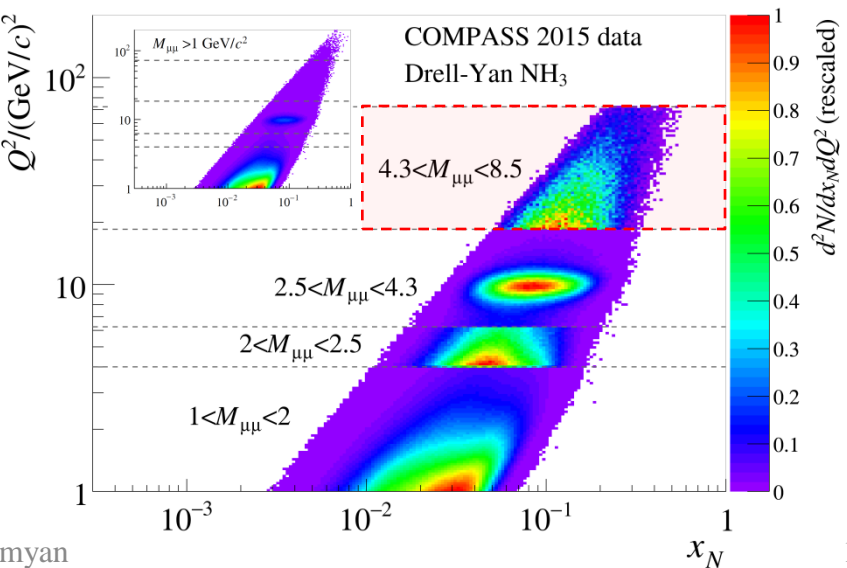
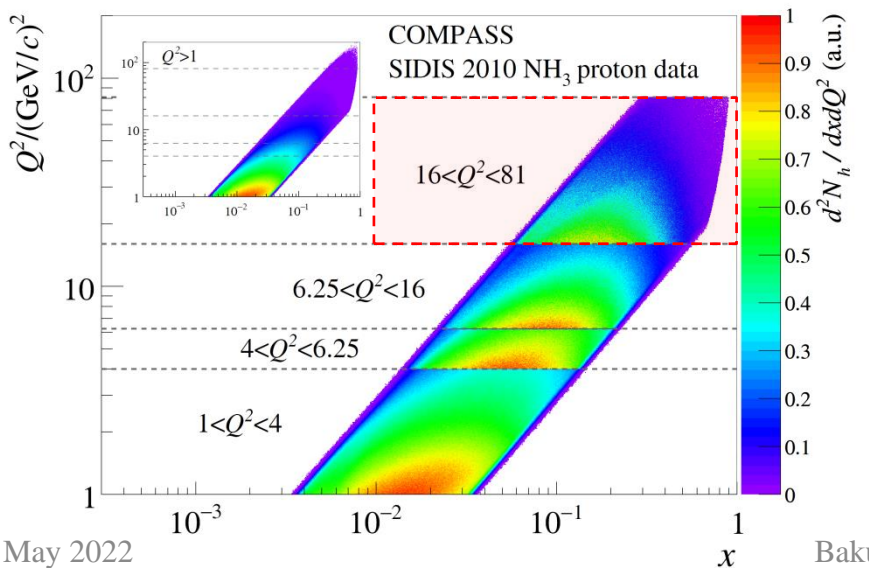
$$\times \left\{ \begin{array}{l} 1 + \varepsilon A_{UU}^{\cos 2\phi_h} \cos 2\phi_h \\ + S_L \varepsilon A_{UL}^{\sin 2\phi_h} \sin 2\phi_h + S_L \lambda \sqrt{1 - \varepsilon^2} A_{LL} \\ \\ + S_T \left[\begin{array}{l} A_{UT}^{\sin(\phi_h - \phi_S)} \sin(\phi_h - \phi_S) \\ + \varepsilon A_{UT}^{\sin(\phi_h + \phi_S)} \sin(\phi_h + \phi_S) \\ + \varepsilon A_{UT}^{\sin(3\phi_h - \phi_S)} \sin(3\phi_h - \phi_S) \end{array} \right] \\ + S_T \lambda \left[\sqrt{(1 - \varepsilon^2)} A_{LT}^{\cos(\phi_h - \phi_S)} \cos(\phi_h - \phi_S) \right] \end{array} \right\}$$

COMPASS
SIDIS-DY
bridge

$$\times \left\{ \begin{array}{l} 1 + D_{[\sin^2 \theta_{CS}]} A_U^{\cos 2\phi_{CS}} \cos 2\phi_{CS} \\ + S_L \sin^2 \theta_{CS} A_L^{\sin 2\phi_{CS}} \sin 2\phi_{CS} \\ \\ + S_T \left[\begin{array}{l} A_T^{\sin \phi_S} \sin \phi_S \\ + D_{[\sin^2 \theta_{CS}]} \left(\begin{array}{l} A_T^{\sin(2\phi_{CS} - \phi_S)} \sin(2\phi_{CS} - \phi_S) \\ + A_T^{\sin(2\phi_{CS} + \phi_S)} \sin(2\phi_{CS} + \phi_S) \end{array} \right) \end{array} \right] \end{array} \right\}$$

$$\text{where } D_{[\sin^2 \theta_{CS}]} = \sin^2 \theta_{CS} / (1 + \cos^2 \theta_{CS})$$

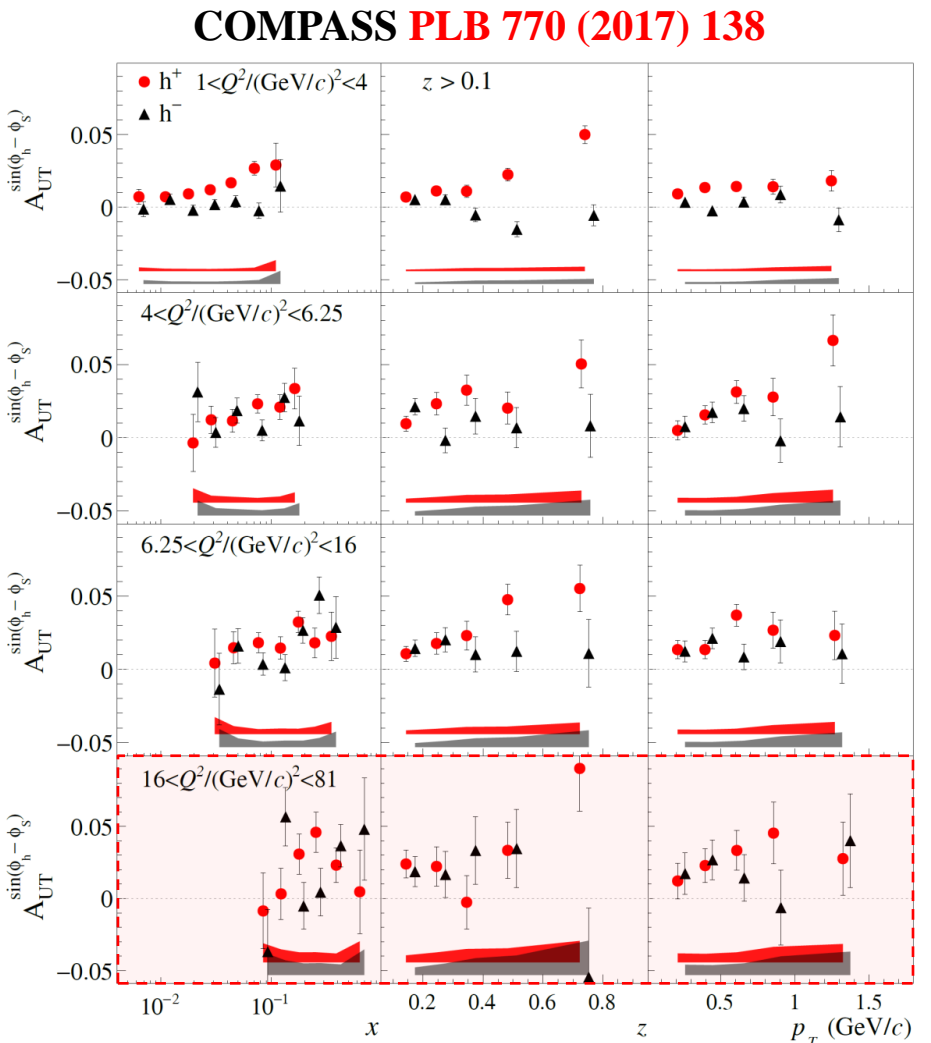
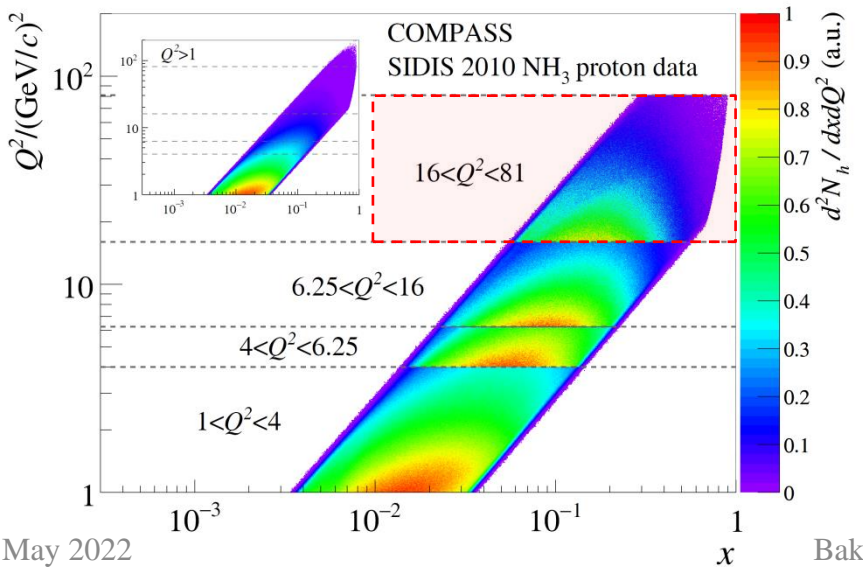
Comparable x:Q² coverage – minimization of possible Q²-evolution effects



SIDIS counterpart: Sivers TSA – 2D analysis

$$\frac{d\sigma^{LO}}{dxdydzdp_T^2 d\phi_h d\phi_S} \propto (F_{UU,T} + \varepsilon F_{UU,L})$$

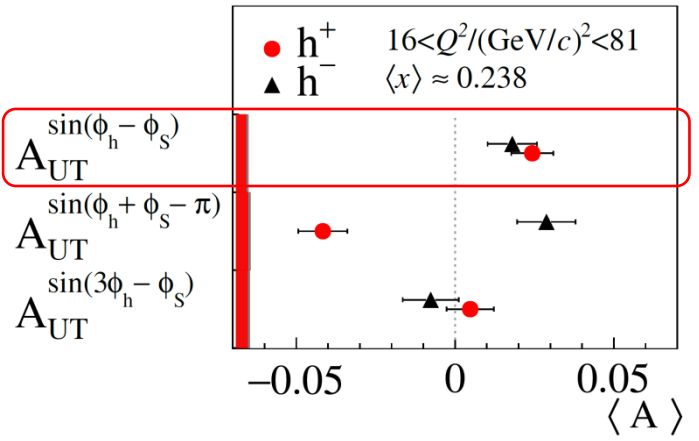
$$\left. \begin{aligned} & 1 + \varepsilon A_{UU}^{\cos 2\phi_h} \cos 2\phi_h \\ & + S_L \varepsilon A_{UL}^{\sin 2\phi_h} \sin 2\phi_h + S_L \lambda \sqrt{1-\varepsilon^2} A_{LL} \\ & \times \left. \begin{aligned} & + S_T \left[\begin{aligned} & A_{UT}^{\sin(\phi_h - \phi_S)} \sin(\phi_h - \phi_S) \\ & + \varepsilon A_{UT}^{\sin(\phi_h + \phi_S)} \sin(\phi_h + \phi_S) \\ & + \varepsilon A_{UT}^{\sin(3\phi_h - \phi_S)} \sin(3\phi_h - \phi_S) \end{aligned} \right] \\ & + S_T \lambda \left[\sqrt{(1-\varepsilon^2)} A_{LT}^{\cos(\phi_h - \phi_S)} \cos(\phi_h - \phi_S) \right] \end{aligned} \right\} \end{aligned} \right.$$



SIDIS: twist-2 TSAs – 2D analysis

$$\frac{d\sigma^{LO}}{dxdydzdp_T^2 d\phi_h d\phi_S} \propto (F_{UU,T} + \varepsilon F_{UU,L})$$

$$\left. \begin{aligned} & 1 + \boxed{\varepsilon A_{UU}^{\cos 2\phi_h} \cos 2\phi_h} \\ & + S_L \varepsilon A_{UL}^{\sin 2\phi_h} \sin 2\phi_h + S_L \lambda \sqrt{1-\varepsilon^2} A_{LL} \\ & \times \left\{ \begin{aligned} & + S_T \left[\begin{aligned} & A_{UT}^{\sin(\phi_h - \phi_S)} \sin(\phi_h - \phi_S) \\ & + \varepsilon A_{UT}^{\sin(\phi_h + \phi_S)} \sin(\phi_h + \phi_S) \\ & + \varepsilon A_{UT}^{\sin(3\phi_h - \phi_S)} \sin(3\phi_h - \phi_S) \end{aligned} \right] \\ & + S_T \lambda \left[\sqrt{(1-\varepsilon^2)} A_{LT}^{\cos(\phi_h - \phi_S)} \cos(\phi_h - \phi_S) \right] \end{aligned} \right\} \end{aligned} \right\}$$



Single-polarized DY measurements at COMPASS

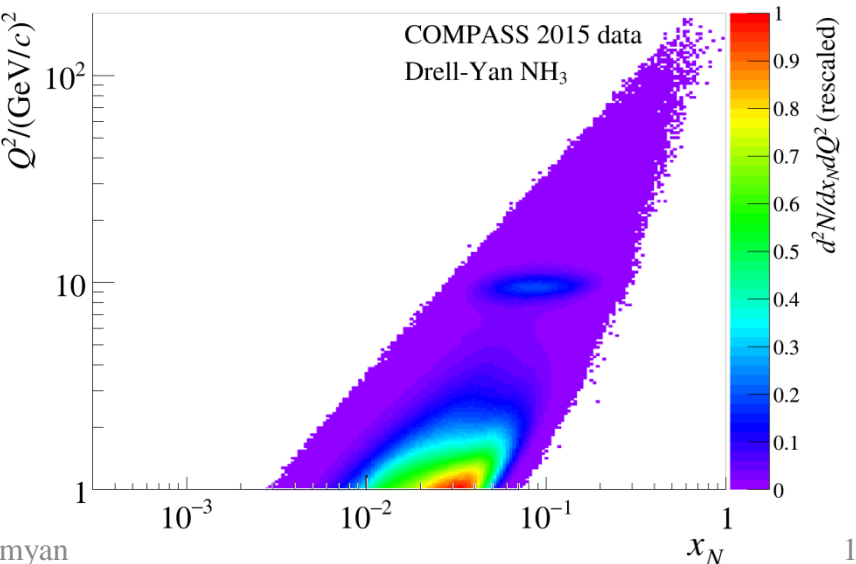
- $1.0 < M /(\text{GeV}/c^2) < 2.0$ “Low mass”
 - Large background contamination, combinatorial, Open-charm (B) $D\bar{D}$, $B\bar{B}$, π , K decays
- $2.0 < M /(\text{GeV}/c^2) < 2.5$ “Intermediate mass”
 - High DY-cross section
 - Still low DY-signal/background ratio
- $2.5 < M /(\text{GeV}/c^2) < 4.3$ “Charmonia mass”
 - Strong J/ ψ -signal → study of J/ ψ physics
 - Good signal/background
- $4.3 < M /(\text{GeV}/c^2) < 8.5$ “High mass”
 - Low DY cross-section
 - Beyond charmonium region, background < 3%
 - Valence region → largest asymmetries

$$\frac{d\sigma^{LO}}{dq^4 d\Omega} \propto F_U^1 \left(1 + \cos^2 \theta_{CS} \right)$$

$$= \left\{ \begin{array}{l} 1 + D_{[\sin^2 \theta_{CS}]} A_U^{\cos 2\varphi_{CS}} \cos 2\varphi_{CS} \\ + S_L \sin^2 \theta_{CS} A_L^{\sin^2 \varphi_{CS}} \sin 2\varphi_{CS} \\ \times \left[A_T^{\sin \varphi_S} \sin \varphi_S \right. \\ \left. + S_T \left[+ D_{[\sin^2 \theta_{CS}]} \left(A_T^{\sin(2\varphi_{CS} - \varphi_S)} \sin(2\varphi_{CS} - \varphi_S) \right. \right. \right. \\ \left. \left. \left. + A_T^{\sin(2\varphi_{CS} + \varphi_S)} \sin(2\varphi_{CS} + \varphi_S) \right) \right] \right] \end{array} \right\}$$

$$D_{[\sin^2 \theta_{CS}]} = \sin^2 \theta_{CS} / (1 + \cos^2 \theta_{CS})$$

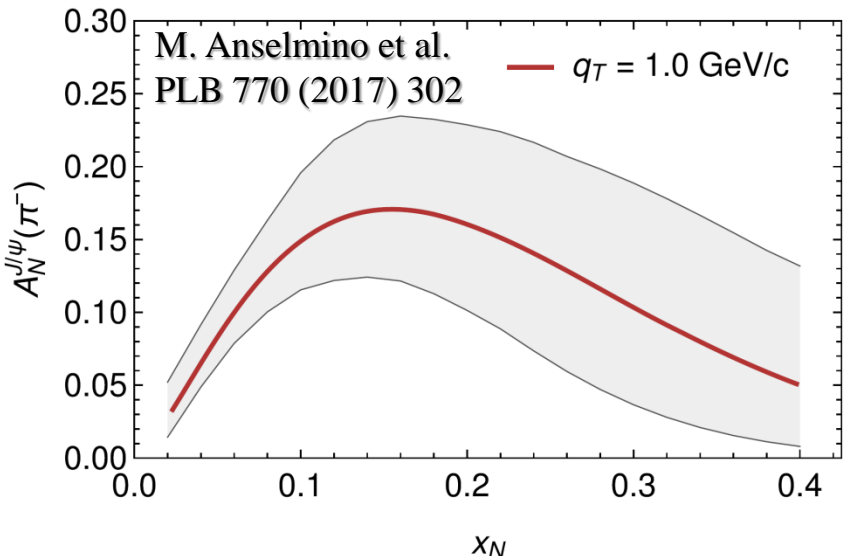
COMPASS x:Q² phase space



Single-polarized DY measurements at COMPASS

- $1.0 < M /(\text{GeV}/c^2) < 2.0$ “Low mass”
 - Large background contamination, combinatorial, Open-charm (B) $D\bar{D}$, $B\bar{B}$, π , K decays
- $2.0 < M /(\text{GeV}/c^2) < 2.5$ “Intermediate mass”
 - High DY-cross section
 - Still low DY-signal/background ratio
- $2.5 < M /(\text{GeV}/c^2) < 4.3$ “Charmonia mass”
 - Strong J/ ψ -signal → study of J/ ψ physics
 - Good signal/background
- $4.3 < M /(\text{GeV}/c^2) < 8.5$ “High mass”
 - Low DY cross-section
 - Beyond charmonium region, background < 3%
 - Valence region → largest asymmetries

$$\langle x_\pi \rangle = 0.31, \langle x_N \rangle = 0.09, \langle x_F \rangle = 0.22, \langle q_T \rangle = 1.1 \text{ GeV}/c$$

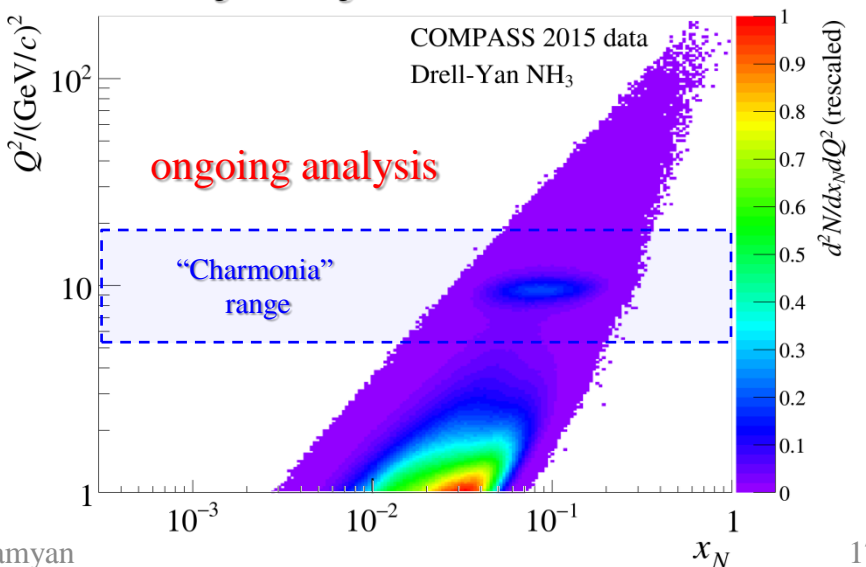


$$\frac{d\sigma^{LO}}{dq^4 d\Omega} \propto F_U^1 \left(1 + \cos^2 \theta_{CS} \right)$$

$$\times \left\{ \begin{array}{l} 1 + D_{[\sin^2 \theta_{CS}]} A_U^{\cos 2\varphi_{CS}} \cos 2\varphi_{CS} \\ + S_L \sin^2 \theta_{CS} A_L^{\sin^2 \varphi_{CS}} \sin 2\varphi_{CS} \\ \times \left[\begin{array}{l} A_T^{\sin \varphi_S} \sin \varphi_S \\ + S_T \left[\begin{array}{l} + D_{[\sin^2 \theta_{CS}]} \left(A_T^{\sin(2\varphi_{CS} - \varphi_S)} \sin(2\varphi_{CS} - \varphi_S) \right. \right. \\ \left. \left. + A_T^{\sin(2\varphi_{CS} + \varphi_S)} \sin(2\varphi_{CS} + \varphi_S) \right) \right] \end{array} \right] \end{array} \right\}$$

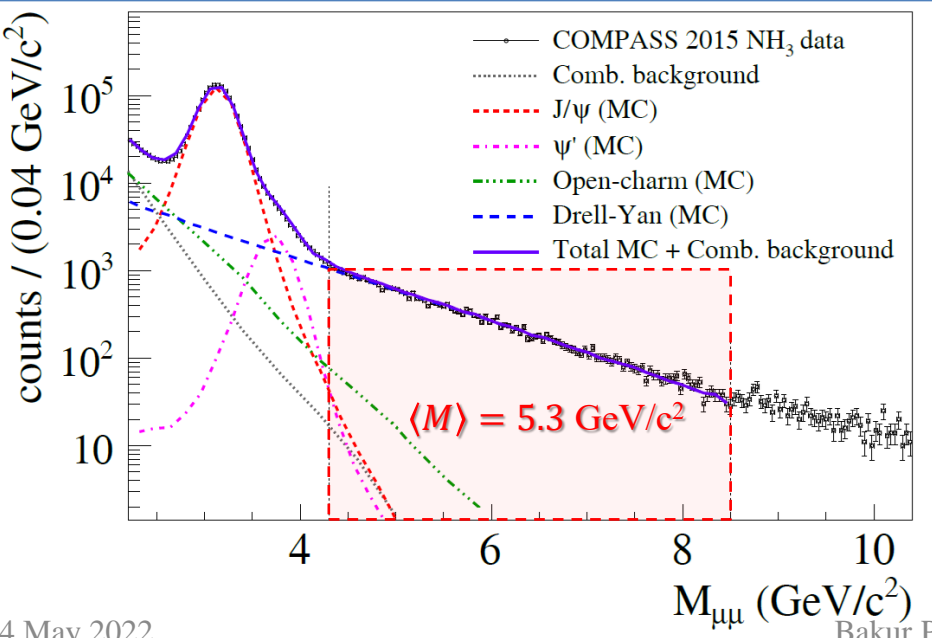
$$D_{[\sin^2 \theta_{CS}]} = \sin^2 \theta_{CS} / (1 + \cos^2 \theta_{CS})$$

$2.5 < M /(\text{GeV}/c^2) < 4.3$ “Charmonia mass”
Strong J/ ψ -signal → study of J/ ψ physics
Good signal/background



Single-polarized DY measurements at COMPASS

- $1.0 < M / (\text{GeV}/c^2) < 2.0$ “Low mass”
 - Large background contamination, combinatorial, Open-charm (B) $D\bar{D}$, $B\bar{B}$, π , K decays
- $2.0 < M / (\text{GeV}/c^2) < 2.5$ “Intermediate mass”
 - High DY-cross section
 - Still low DY-signal/background ratio
- $2.5 < M / (\text{GeV}/c^2) < 4.3$ “Charmonia mass”
 - Strong J/ ψ -signal → study of J/ ψ physics
 - Good signal/background
- $4.3 < M / (\text{GeV}/c^2) < 8.5$ “High mass”
 - Low DY cross-section
 - Beyond charmonium region, background $< 3\%$
 - Valence region → largest asymmetries



$$\frac{d\sigma^{LO}}{dq^4 d\Omega} \propto F_U^1 \left(1 + \cos^2 \theta_{CS} \right)$$

$$\times \left\{ 1 + D_{[\sin^2 \theta_{CS}]} A_U^{\cos 2\varphi_{CS}} \cos 2\varphi_{CS} \right.$$

$$\left. + S_L \sin^2 \theta_{CS} A_L^{\sin^2 \varphi_{CS}} \sin 2\varphi_{CS} \right\}$$

$$\times \left\{ A_T^{\sin \varphi_S} \sin \varphi_S \right.$$

$$\left. + S_T \left[+ D_{[\sin^2 \theta_{CS}]} \left(A_T^{\sin(2\varphi_{CS} - \varphi_S)} \sin(2\varphi_{CS} - \varphi_S) \right. \right. \right.$$

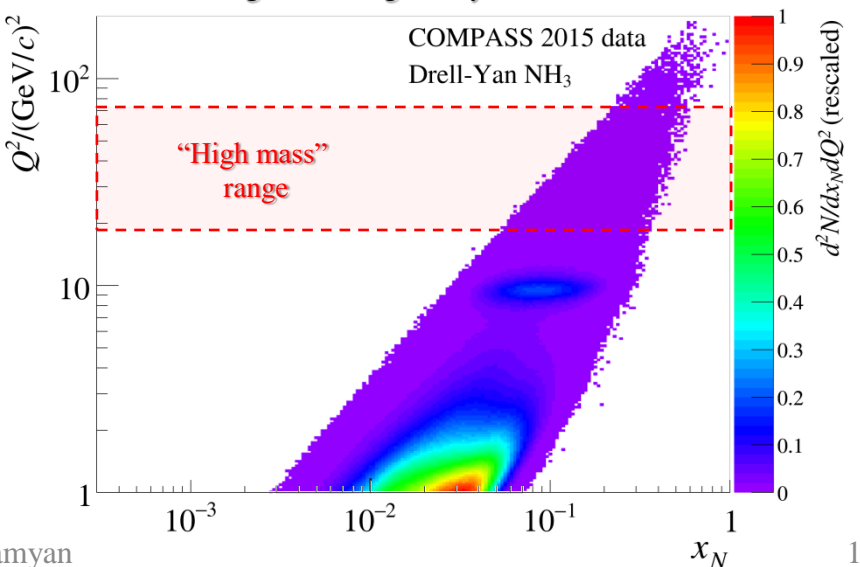
$$\left. \left. \left. + A_T^{\sin(2\varphi_{CS} + \varphi_S)} \sin(2\varphi_{CS} + \varphi_S) \right) \right] \right\}$$

$$D_{[\sin^2 \theta_{CS}]} = \sin^2 \theta_{CS} / (1 + \cos^2 \theta_{CS})$$

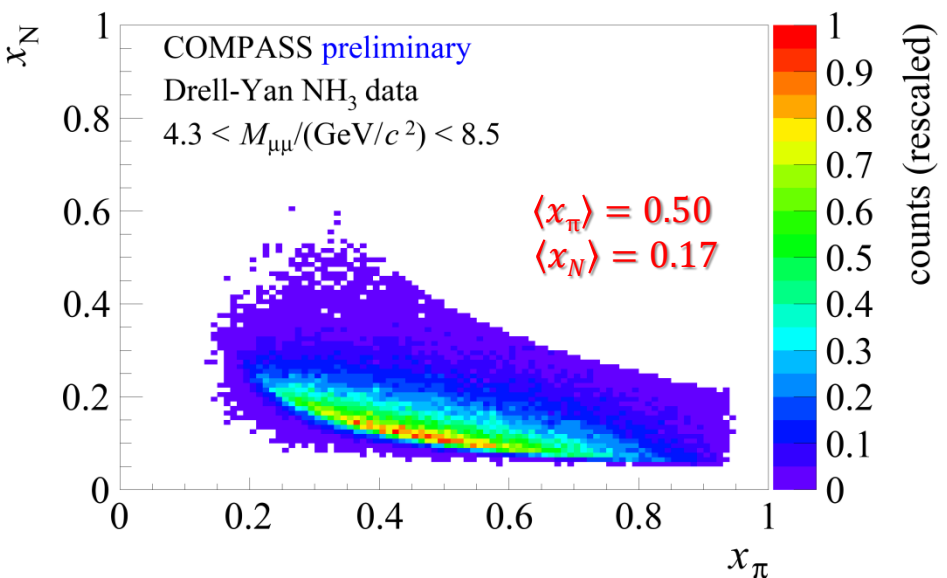
$4.3 < M / (\text{GeV}/c^2) < 8.5$ “High mass” range

Beyond charmonium region, background $< 3\%$

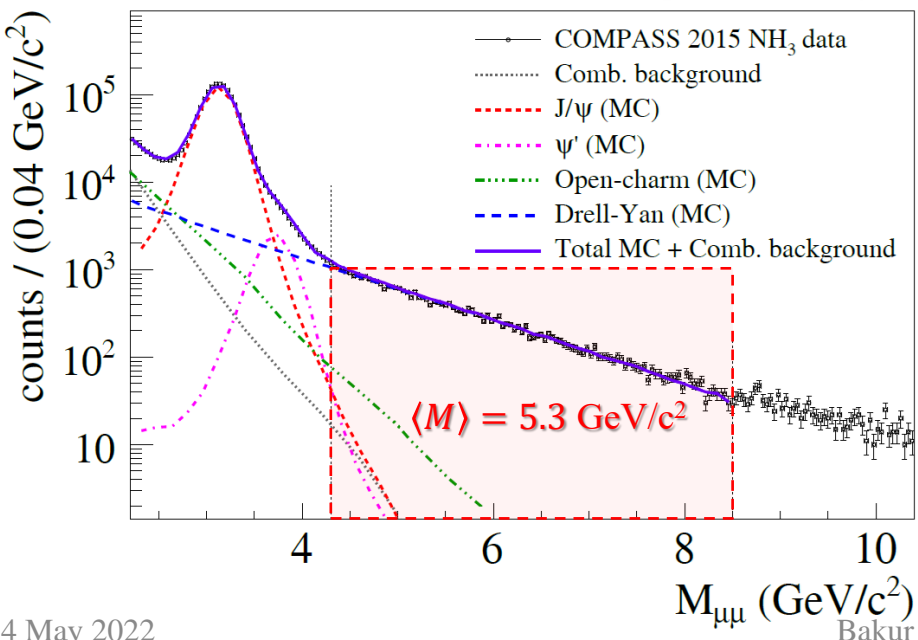
Valence region → largest asymmetries



Single-polarized DY measurements at COMPASS



HM events are in the valence quark range



$$\frac{d\sigma^{LO}}{dq^4 d\Omega} \propto F_U^1 \left(1 + \cos^2 \theta_{CS} \right)$$

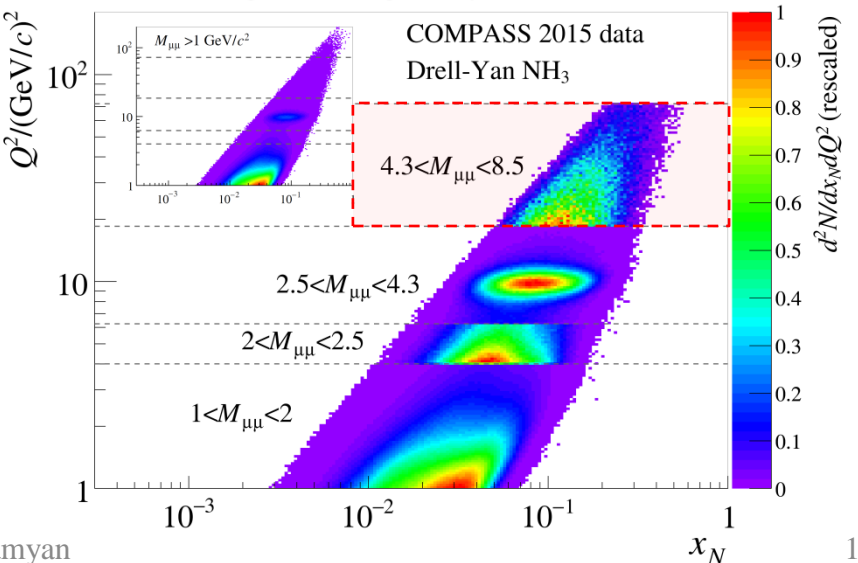
$$\times \begin{cases} 1 + D_{[\sin^2 \theta_{CS}]} A_U^{\cos 2\varphi_{CS}} \cos 2\varphi_{CS} \\ + S_L \sin^2 \theta_{CS} A_L^{\sin^2 \varphi_{CS}} \sin 2\varphi_{CS} \\ + S_T \left[A_T^{\sin \varphi_S} \sin \varphi_S \right. \\ \left. + D_{[\sin^2 \theta_{CS}]} \left(A_T^{\sin(2\varphi_{CS} - \varphi_S)} \sin(2\varphi_{CS} - \varphi_S) \right. \right. \\ \left. \left. + A_T^{\sin(2\varphi_{CS} + \varphi_S)} \sin(2\varphi_{CS} + \varphi_S) \right) \right] \end{cases}$$

$$D_{[\sin^2 \theta_{CS}]} = \sin^2 \theta_{CS} / (1 + \cos^2 \theta_{CS})$$

$4.3 < M / (\text{GeV}/c^2) < 8.5$ “High mass” range

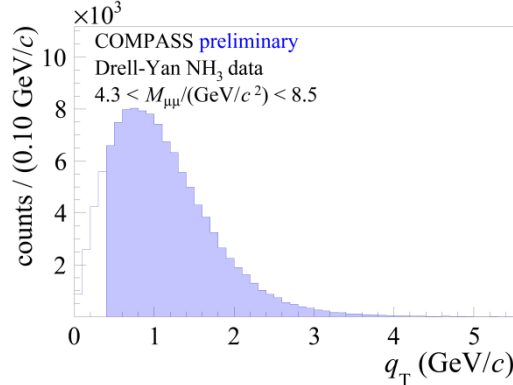
Beyond charmonium region, background < 3%

Valence region → largest asymmetries



Single-polarized DY measurements at COMPASS

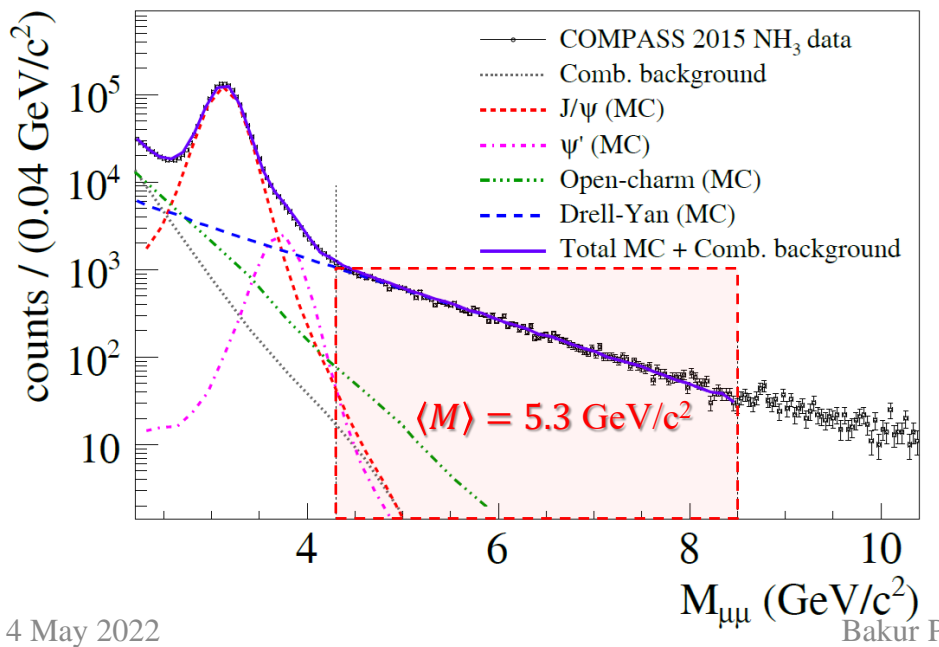
Dimuon transverse momentum $q_T > 0.4 \text{ GeV}/c$
 $\langle x_F \rangle = 0.33, \langle q_T \rangle = 1.2 \text{ GeV}/c$



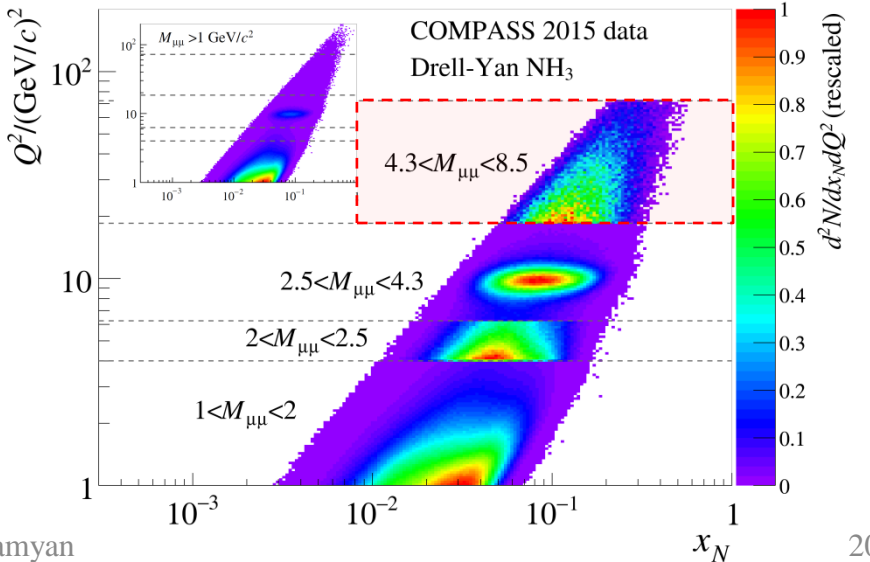
$$\frac{d\sigma^{LO}}{dq^4 d\Omega} \propto F_U^1 (1 + \cos^2 \theta_{CS})$$

$$\begin{aligned} & 1 + D_{[\sin^2 \theta_{CS}]} A_U^{\cos 2\varphi_{CS}} \cos 2\varphi_{CS} \\ & + S_L \sin^2 \theta_{CS} A_L^{\sin^2 \varphi_{CS}} \sin 2\varphi_{CS} \\ & + S_T \left[A_T^{\sin \varphi_S} \sin \varphi_S \right. \\ & \quad \left. + D_{[\sin^2 \theta_{CS}]} \left(A_T^{\sin(2\varphi_{CS}-\varphi_S)} \sin(2\varphi_{CS}-\varphi_S) \right. \right. \\ & \quad \left. \left. + A_T^{\sin(2\varphi_{CS}+\varphi_S)} \sin(2\varphi_{CS}+\varphi_S) \right) \right] \end{aligned}$$

$$D_{[\sin^2 \theta_{CS}]} = \sin^2 \theta_{CS} / (1 + \cos^2 \theta_{CS})$$

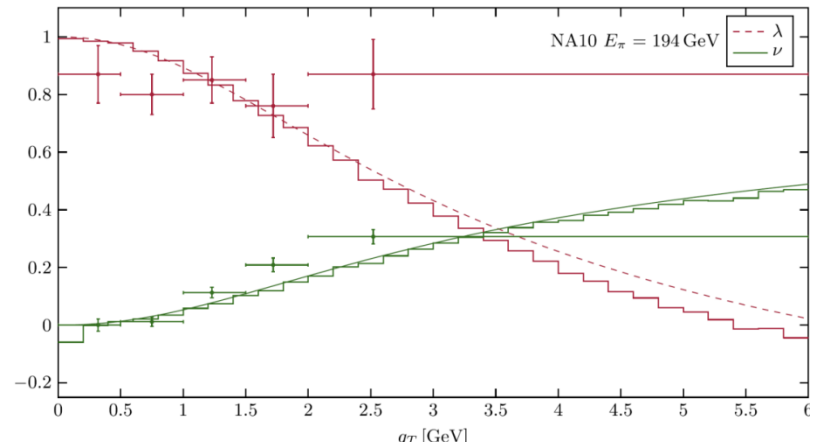


$4.3 < M / (\text{GeV}/c^2) < 8.5$ “High mass” range
 Beyond charmonium region, background < 3%
 Valence region → largest asymmetries



Single-polarized DY x-section: transverse part

M. Lambertsen, W. Vogelsang PRD93, 114013 (2016)



$$\lambda = A_U^1, \mu = A_U^{\cos \varphi_{CS}}, \nu = 2A_U^{\cos 2\varphi_{CS}}$$

- “naive” Drell–Yan model
collinear ($k_T=0$) LO pQCD no rad. processes
 $\lambda=1$, $(F_U^2=0)$, $\mu=\nu=0$
- Intrinsic transverse motion + QCD effects
 $\lambda \neq 1$, $\mu \neq 0$, $\nu \neq 0$ but $1-\lambda=2\nu$ (Lam-Tung)
- Experiment,
 $\lambda \neq 1$, $\mu \neq 0$, $\nu \neq 0$

$$\frac{d\sigma}{d\Omega} \propto (F_U^1 + F_U^2)(1 + A_U^1 \cos^2 \theta_{CS})$$

$$\times \left\{ 1 + D_{[\sin^2 \theta_{CS}]} A_U^{\cos 2\varphi_{CS}} \cos 2\varphi_{CS} + D_{[\sin 2\theta_{CS}]} A_U^{\cos \varphi_{CS}} \cos \varphi_{CS} \right.$$

$$\left. + S_T \begin{bmatrix} A_T^{\sin \varphi_s} \sin \varphi_s \\ + D_{[\sin 2\theta_{CS}]} \left(A_T^{\sin(\varphi_{CS}-\varphi_s)} \sin(\varphi_{CS}-\varphi_s) \right. \\ \left. + A_T^{\sin(\varphi_{CS}+\varphi_s)} \sin(\varphi_{CS}+\varphi_s) \right) \\ + D_{[\sin^2 \theta_{CS}]} \left(A_T^{\sin(2\varphi_{CS}-\varphi_s)} \sin(2\varphi_{CS}-\varphi_s) \right. \\ \left. + A_T^{\sin(2\varphi_{CS}+\varphi_s)} \sin(2\varphi_{CS}+\varphi_s) \right) \end{bmatrix} \right\}$$

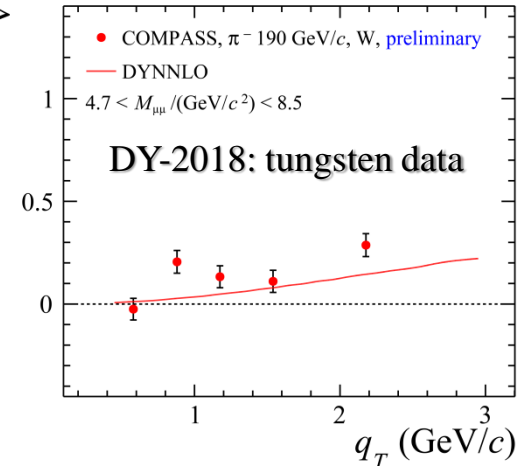
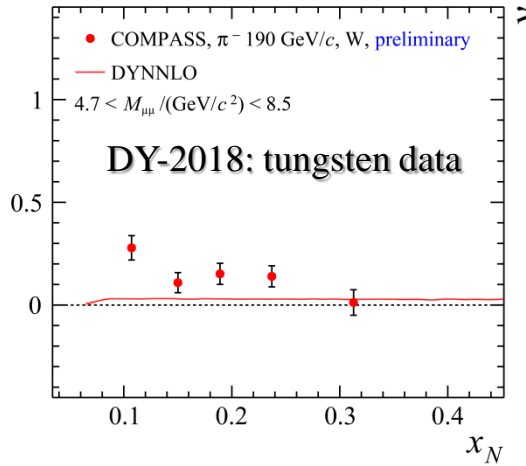
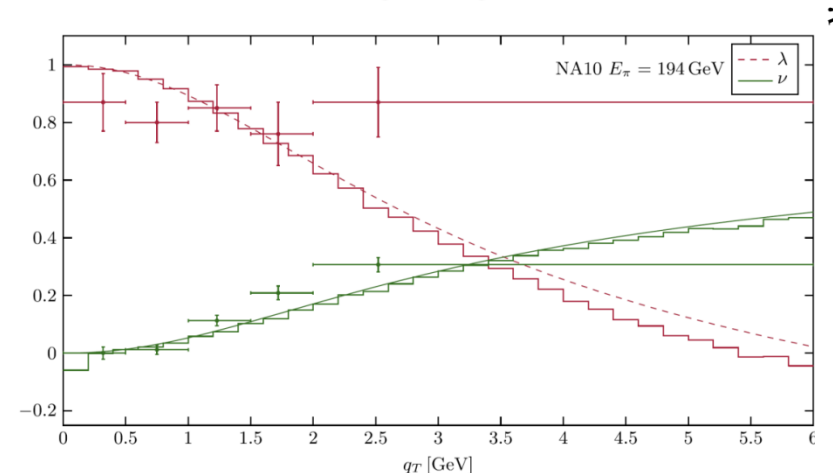
$$D_{[f(\theta_{CS})]} = f(\theta_{CS}) / (1 + A_U^1 \cos^2 \theta_{CS})$$

- All five Drell-Yan TSAs are extracted simultaneously using extended unbinned Maximum likelihood estimator.
- Depolarization factors are evaluated under assumption $A_U^1=1$

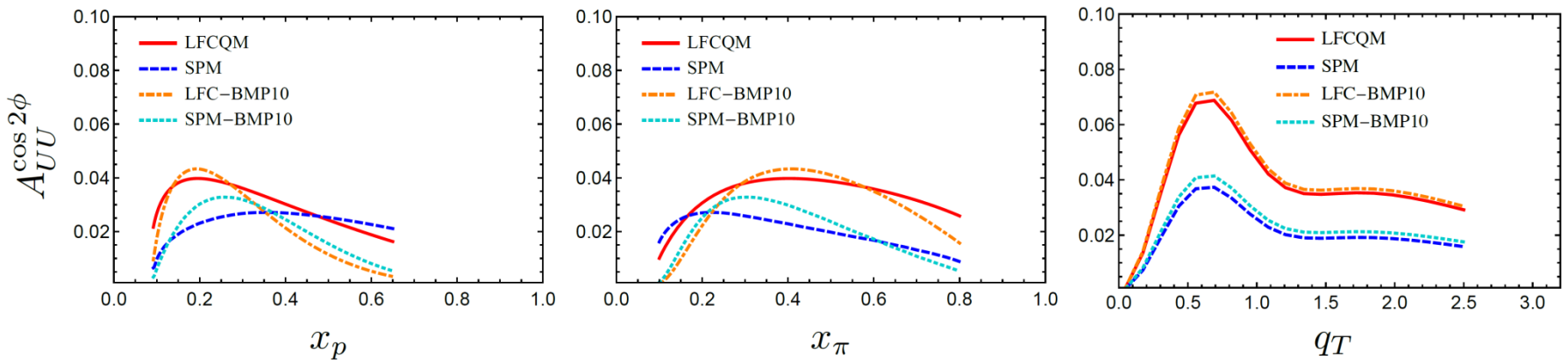
Unpolarized Drell-Yan results (high-mass range)

M. Lambertsen, W. Vogelsang PRD93, 114013 (2016)

Preliminary results Released for DIS-2021

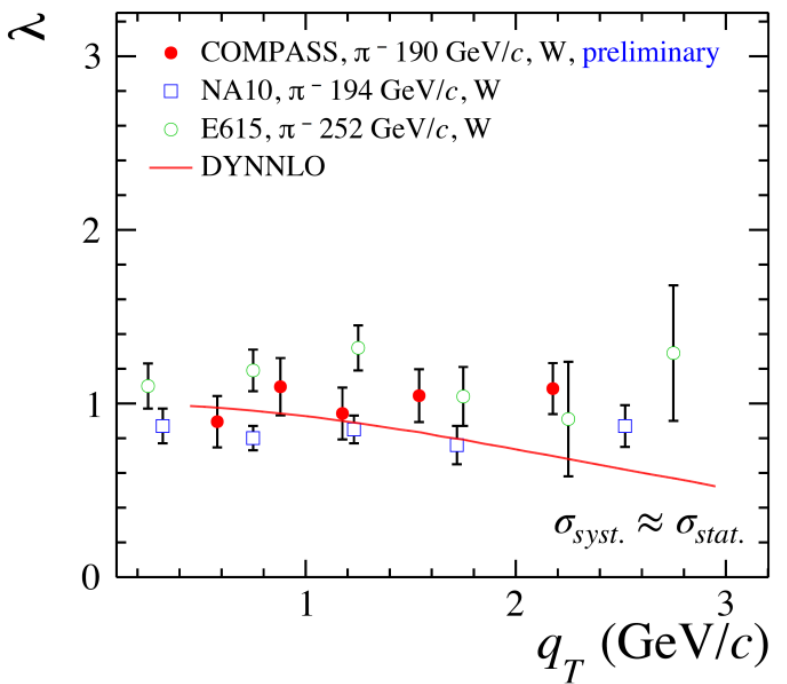
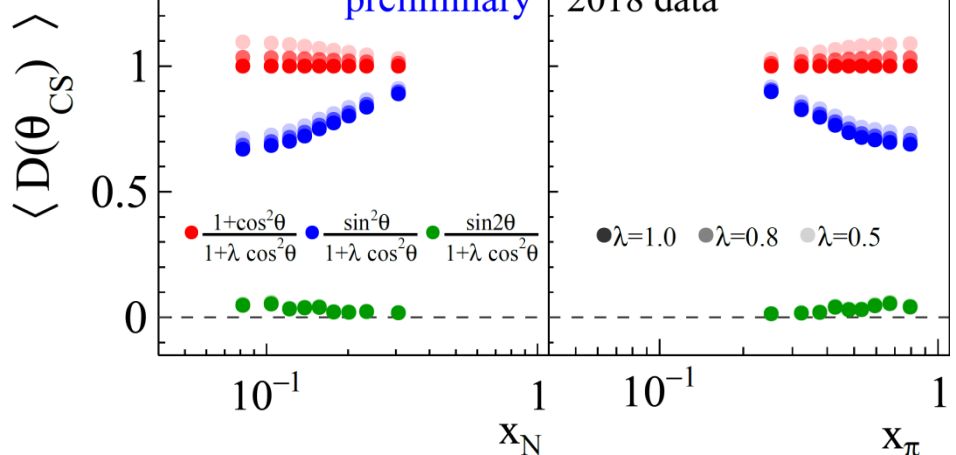


S. Bastami et al. JHEP 02, (2021), 166



Is there a room for BM at low (COMPASS) q_T ?

Single-polarized DY x-section: transverse part



$$\frac{d\sigma}{d\Omega} \propto (F_U^1 + F_U^2)(1 + A_U^1 \cos^2 \theta_{CS})$$

$$\times \left\{ 1 + D_{[\sin^2 \theta_{CS}]} A_U^{\cos 2\varphi_{CS}} \cos 2\varphi_{CS} + D_{[\sin 2\theta_{CS}]} A_U^{\cos \varphi_{CS}} \cos \varphi_{CS} \right.$$

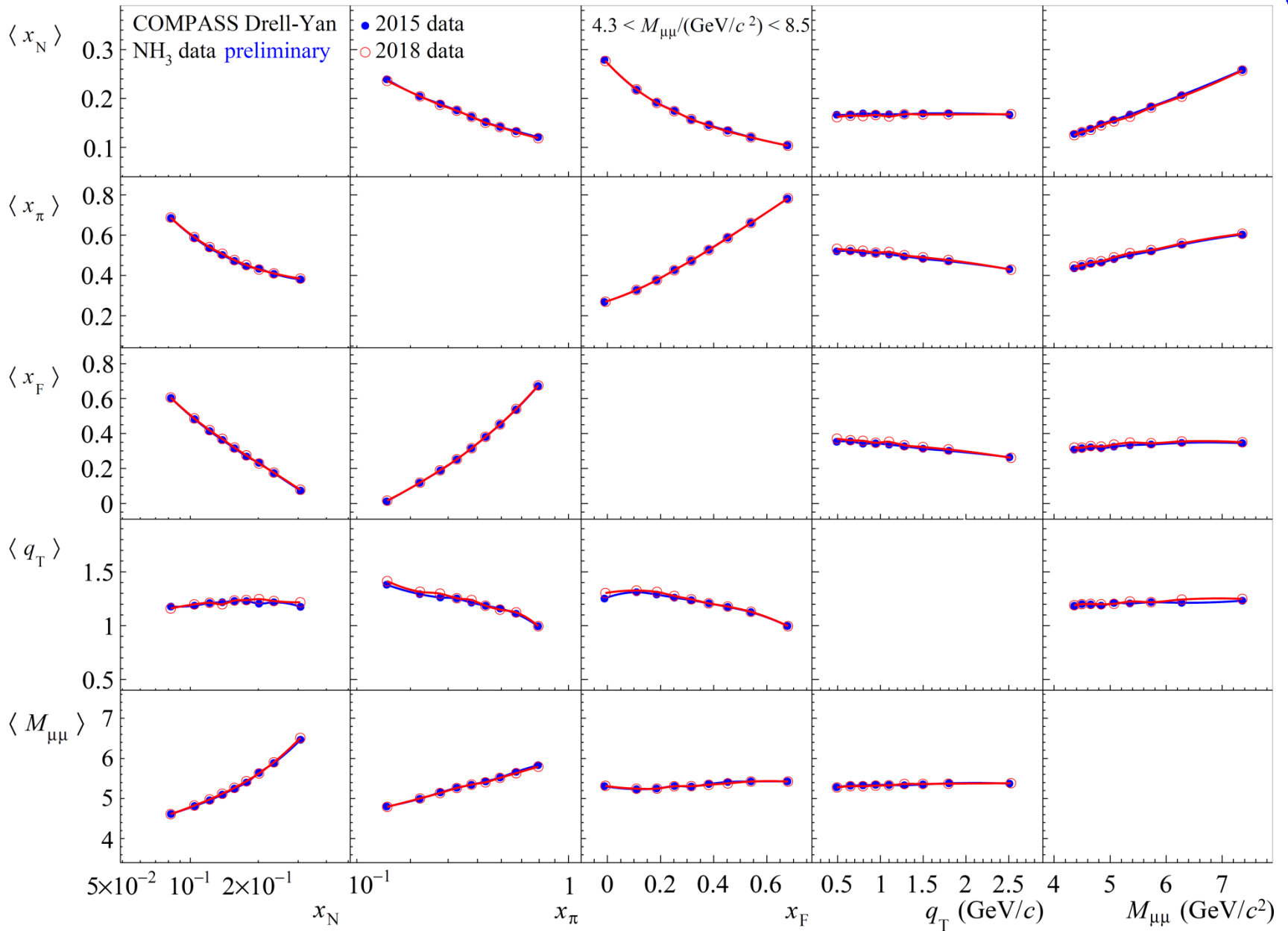
$$\left. + S_T \left[A_T^{\sin \varphi_s} \sin \varphi_s + D_{[\sin 2\theta_{CS}]} \left(A_T^{\sin(\varphi_{CS}-\varphi_s)} \sin(\varphi_{CS}-\varphi_s) + A_T^{\sin(\varphi_{CS}+\varphi_s)} \sin(\varphi_{CS}+\varphi_s) \right) \right. \right.$$

$$\left. \left. + D_{[\sin^2 \theta_{CS}]} \left(A_T^{\sin(2\varphi_{CS}-\varphi_s)} \sin(2\varphi_{CS}-\varphi_s) + A_T^{\sin(2\varphi_{CS}+\varphi_s)} \sin(2\varphi_{CS}+\varphi_s) \right) \right] \right\}$$

$$D_{[f(\theta_{CS})]} = f(\theta_{CS}) / (1 + A_U^1 \cos^2 \theta_{CS})$$

- All five Drell-Yan TSAs are extracted simultaneously using extended unbinned Maximum likelihood estimator.
- Depolarization factors are evaluated under assumption $A_U^1=1$
- Possible impact of $A_U^1 \neq 1$ scenarios lead to a normalization uncertainty of at most -5%.

Kinematic map: high mass range 2015 and 2018 data



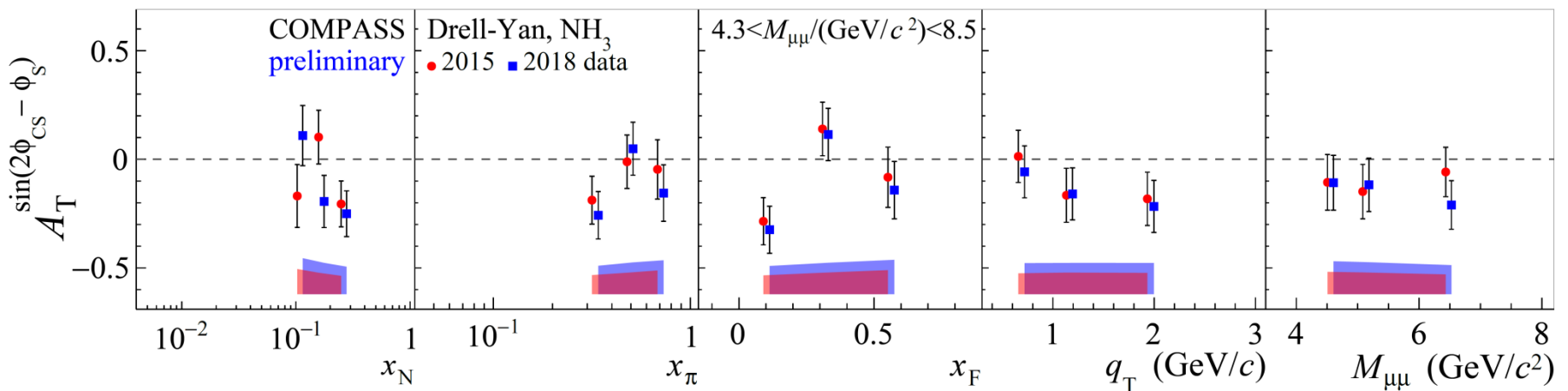
Drell-Yan TSAs – Transversity

$$\frac{d\sigma}{dq^4 d\Omega} \propto 1 + \dots + S_T \left[D_{[\sin^2 \theta_{CS}]} A_T^{\sin(2\phi_{CS} - \phi_s)} \sin(2\phi_{CS} - \phi_s) + \dots \right]$$

COMPASS 2015 + 2018 data **NEW!**

Transversity DY TSA

$$A_T^{\sin(2\phi_{CS} - \phi_s)} \propto h_{1,\pi}^{\perp q} \otimes h_{1,p}^q$$



- Full re-processing and re-analysis of both 2015 and 2018 samples
- Results from 2015 and 2018 samples are in agreement
 - Somewhat larger systematics for 2018 sample
- Combined TSAs from 2015 and 2018 are presented – **NEW!**

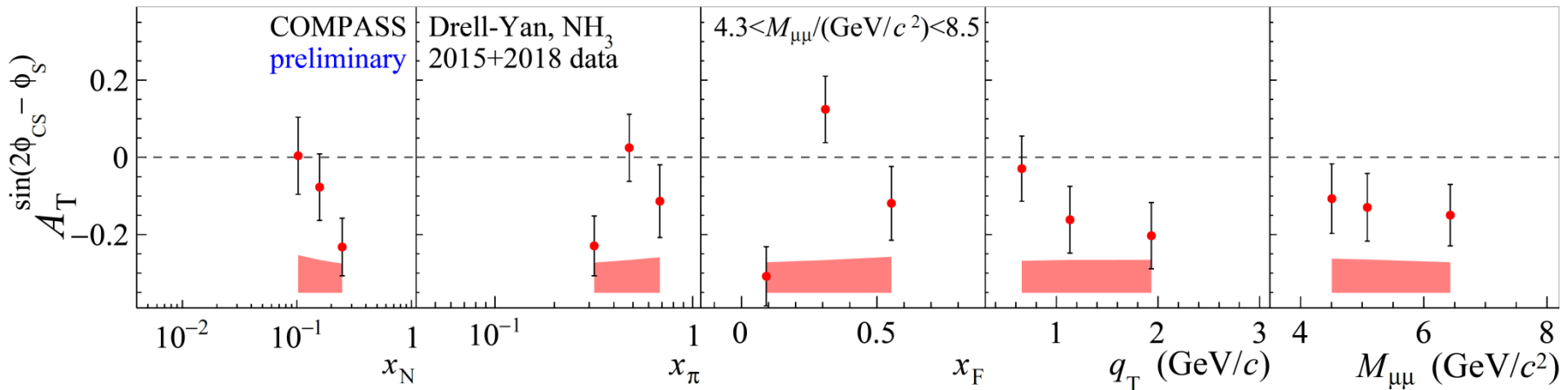
Drell-Yan TSAs – Transversity

$$\frac{d\sigma}{dq^4 d\Omega} \propto 1 + \dots + S_T \left[D_{[\sin^2 \theta_{CS}]} A_T^{\sin(2\phi_{CS} - \phi_s)} \sin(2\phi_{CS} - \phi_s) + \dots \right]$$

COMPASS 2015 + 2018 data **NEW!**

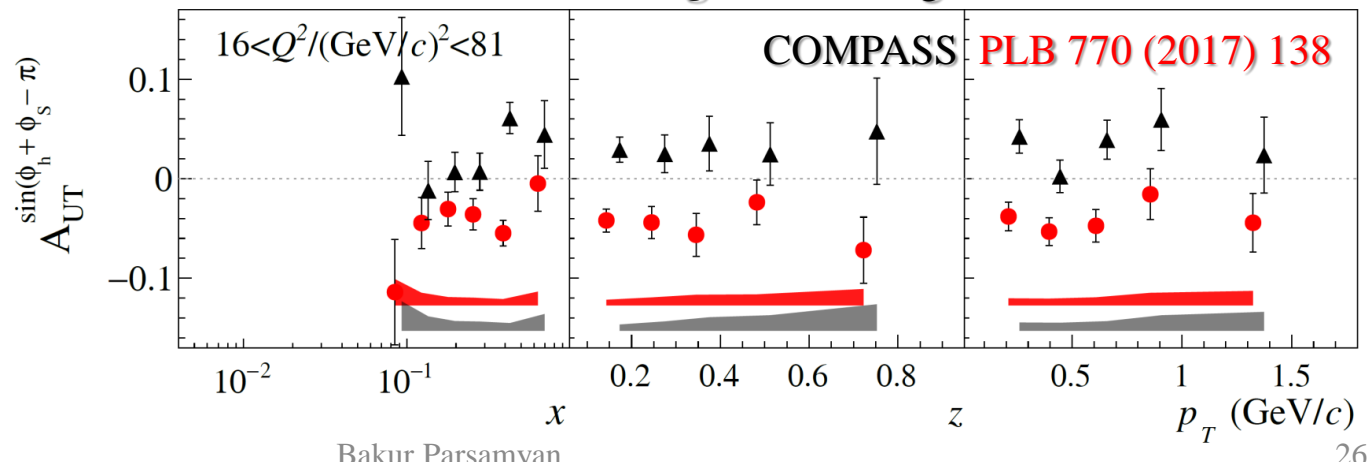
Transversity DY TSA

$$A_T^{\sin(2\phi_{CS} - \phi_s)} \propto h_{1,\pi}^{\perp q} \otimes h_{1,p}^q$$



Collins SIDIS TSA
 $A_{UT}^{\sin(\phi_h + \phi_s)} \propto h_1^q \otimes H_{1q}^{\perp h}$

SIDIS in Drell-Yan *high-mass range*



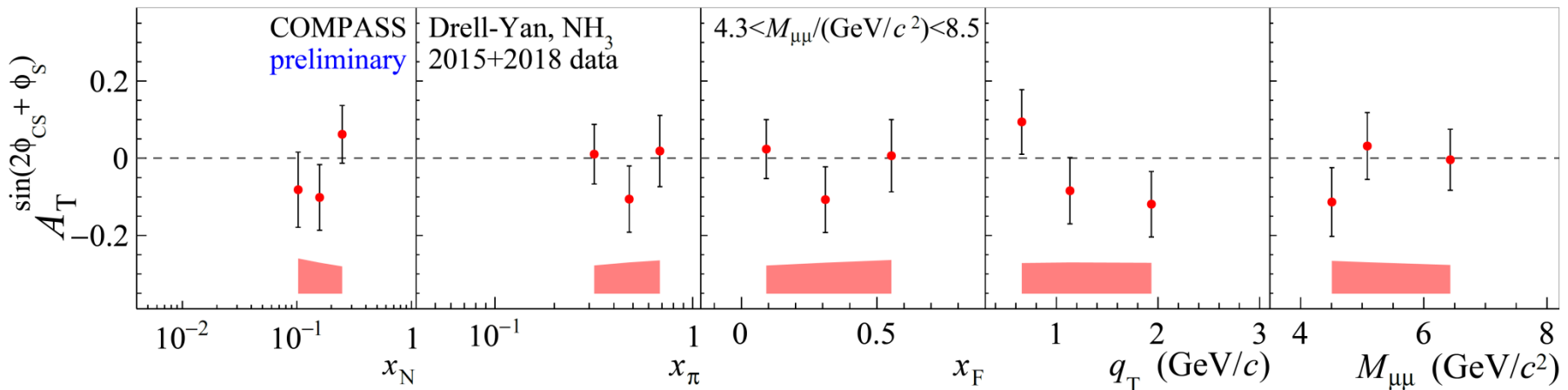
Drell-Yan TSAs – Pretzelosity

$$\frac{d\sigma}{dq^4 d\Omega} \propto 1 + \dots + S_T \left[D_{[\sin^2 \theta_{CS}]} A_T^{\sin(2\phi_{CS} + \phi_s)} \sin(2\phi_{CS} - \phi_s) + \dots \right]$$

COMPASS 2015 + 2018 data **NEW!**

Pretzelosity DY TSA

$$A_T^{\sin(2\phi_{CS} + \phi_s)} \propto h_{1,\pi}^{\perp q} \otimes h_{1T,p}^{\perp q}$$

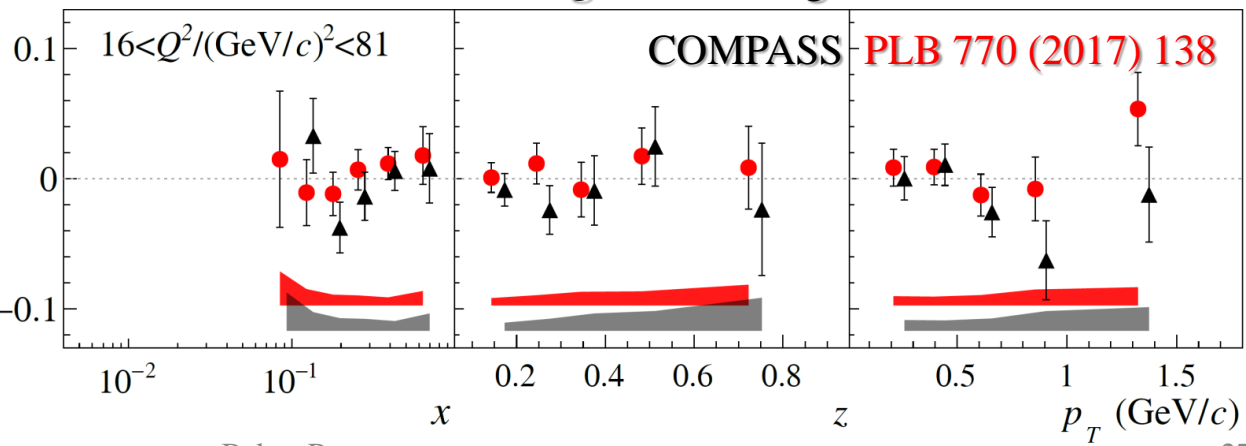


SIDIS in Drell-Yan *high-mass range*

Pretzelosity SIDIS TSA

$$A_{UT}^{\sin(3\phi_h - \phi_s)} \propto h_{1T}^{\perp q} \otimes H_{1q}^{\perp h}$$

$$A_{UT}^{\sin(3\phi_h - \phi_s)}$$



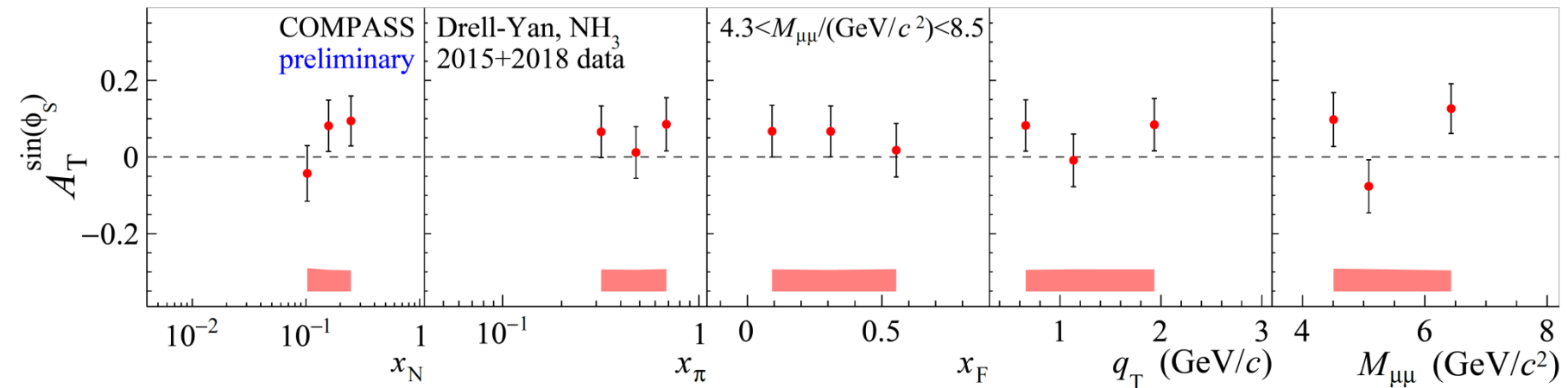
Drell-Yan TSAs – Sivers

$$\frac{d\sigma}{dq^4 d\Omega} \propto 1 + \dots + S_T [A_T^{\sin \varphi_S} \sin \varphi_S + \dots]$$

COMPASS 2015 + 2018 data **NEW!**

Sivers DY TSA

$$A_T^{\sin \varphi_S} \propto f_{1,\pi}^q \otimes f_{1T,p}^{\perp q}$$

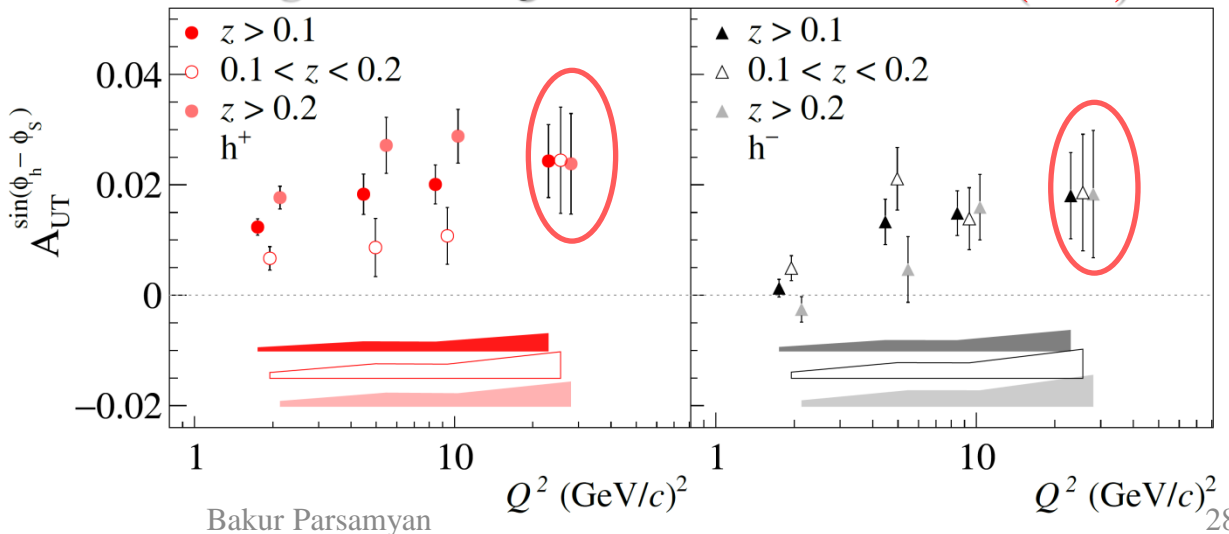


SIDIS in Drell-Yan *high-mass* range

COMPASS **PLB 770 (2017) 138**

Sivers SIDIS TSA

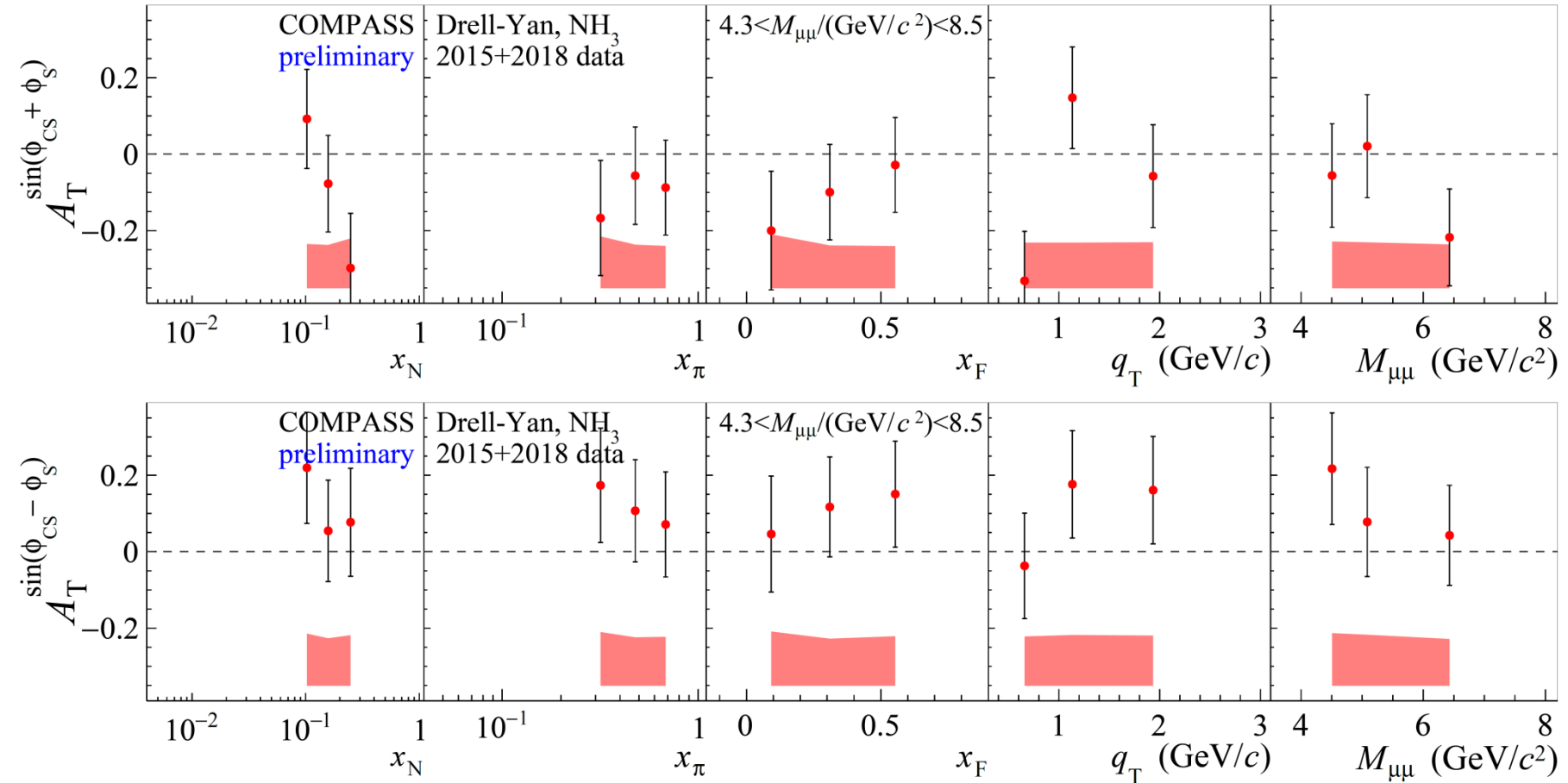
$$A_{UT}^{\sin(\phi_h - \phi_s)} \propto f_{1T}^{\perp q} \otimes D_{1q}^h$$



Drell-Yan TSAs – “higher twists”

$$\frac{d\sigma}{d\Omega} \propto 1 + \dots + S_T \left[D_{[\sin 2\theta_{CS}]} A_T^{\sin(\varphi_{CS} + \varphi_S)} \sin(\varphi_{CS} + \varphi_S) + D_{[\sin 2\theta_{CS}]} A_T^{\sin(\varphi_{CS} - \varphi_S)} \sin(\varphi_{CS} - \varphi_S) \dots \right]$$

COMPASS 2015 + 2018 data **NEW!**



SIDIS and DY TSAs at COMPASS (high-mass range)

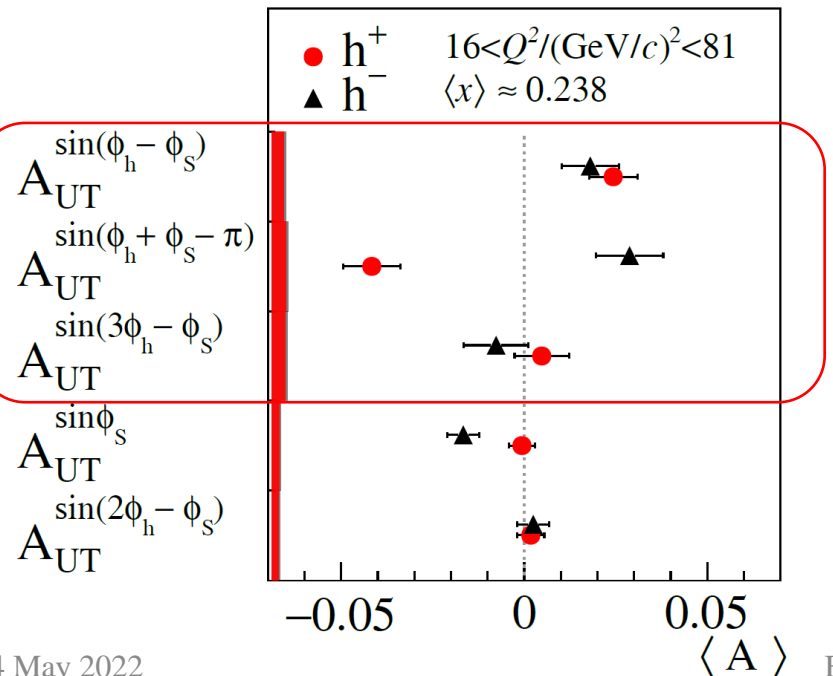
$$\frac{d\sigma}{dxdydzdp_T^2 d\phi_h d\phi_s} \propto (F_{UU,T} + \varepsilon F_{UU,L}) \left\{ 1 + \dots \right.$$

$$+ S_T \left[\begin{array}{l} A_{UT}^{\sin(\phi_h - \phi_s)} \sin(\phi_h - \phi_s) \\ + \varepsilon A_{UT}^{\sin(\phi_h + \phi_s)} \sin(\phi_h + \phi_s) \\ + \varepsilon A_{UT}^{\sin(3\phi_h - \phi_s)} \sin(3\phi_h - \phi_s) \\ + \sqrt{2\varepsilon(1+\varepsilon)} A_{UT}^{\sin\phi_s} \sin\phi_s \\ + \sqrt{2\varepsilon(1+\varepsilon)} A_{UT}^{\sin(2\phi_h - \phi_s)} \sin(2\phi_h - \phi_s) \end{array} \right] \right\}$$

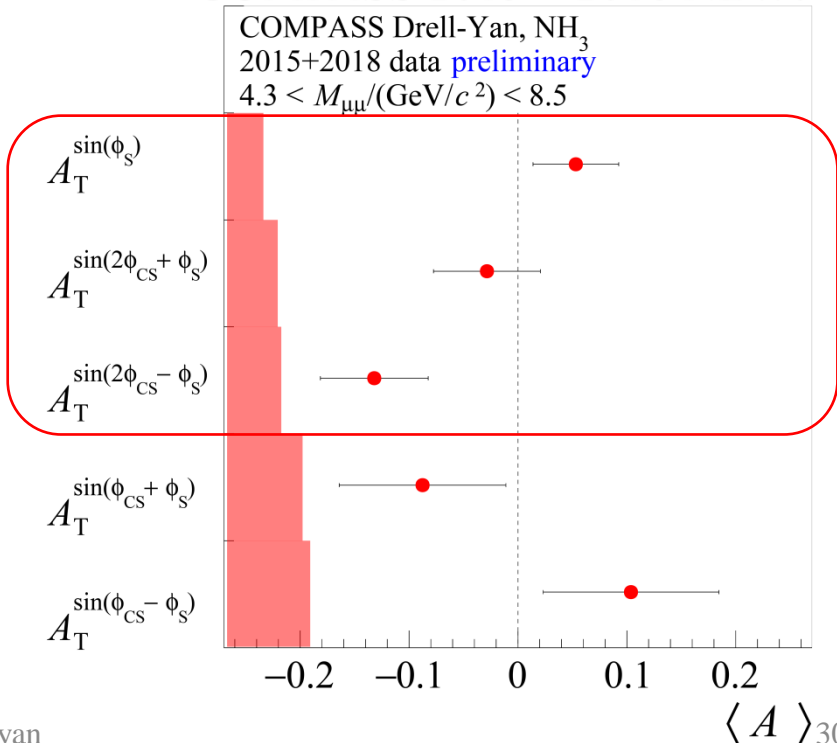
$$\frac{d\sigma^{LO}}{dq^4 d\Omega} \propto F_U^1 (1 + \cos^2 \theta_{CS}) \left\{ 1 + \dots \right.$$

$$+ S_T \left[\begin{array}{l} A_T^{\sin\varphi_s} \sin\varphi_s \\ + D_{[\sin^2 \theta_{CS}]} \left(A_T^{\sin(2\phi_{CS} - \varphi_s)} \sin(2\phi_{CS} - \varphi_s) \right. \\ \left. + A_T^{\sin(2\phi_{CS} + \varphi_s)} \sin(2\phi_{CS} + \varphi_s) \right) \\ + D_{[\sin 2\theta_{CS}]} \left(A_T^{\sin(\phi_{CS} - \varphi_s)} \sin(\phi_{CS} - \varphi_s) \right. \\ \left. + A_T^{\sin(\phi_{CS} + \varphi_s)} \sin(\phi_{CS} + \varphi_s) \right) \end{array} \right] \right\}$$

COMPASS PLB 770 (2017) 138

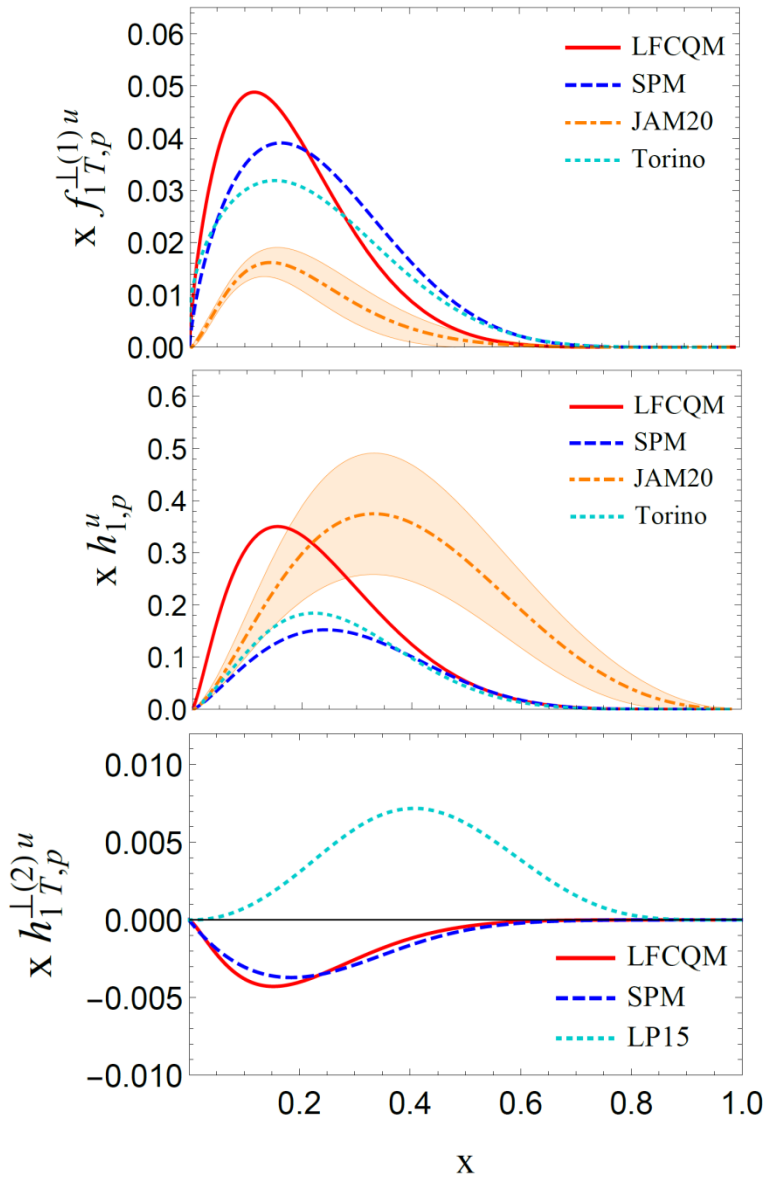


COMPASS 2015 + 2018 NEW!



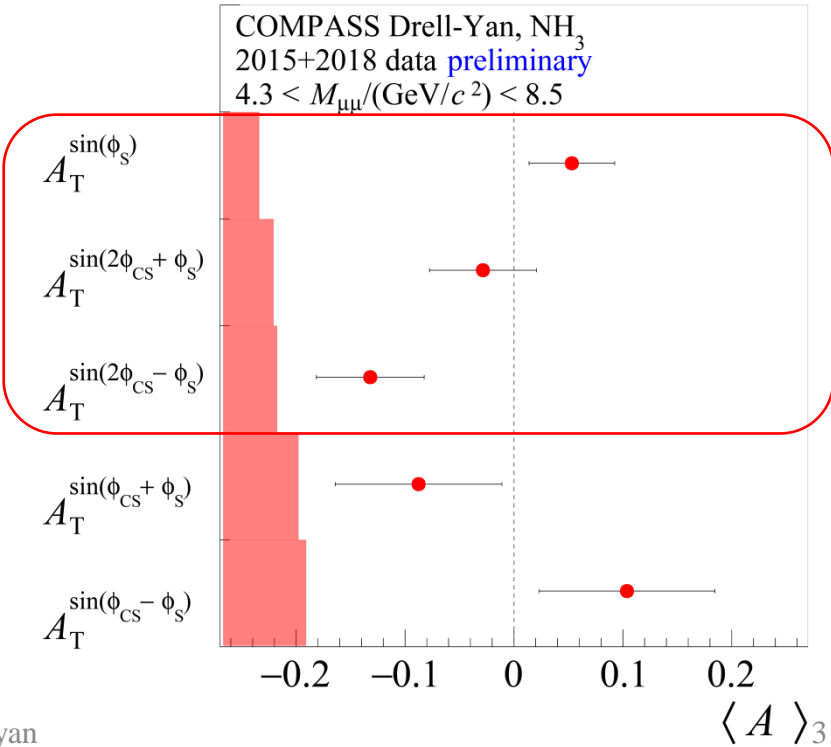
DY TSAs at COMPASS (high-mass range)

S. Bastami et al. JHEP 02, (2021), 166



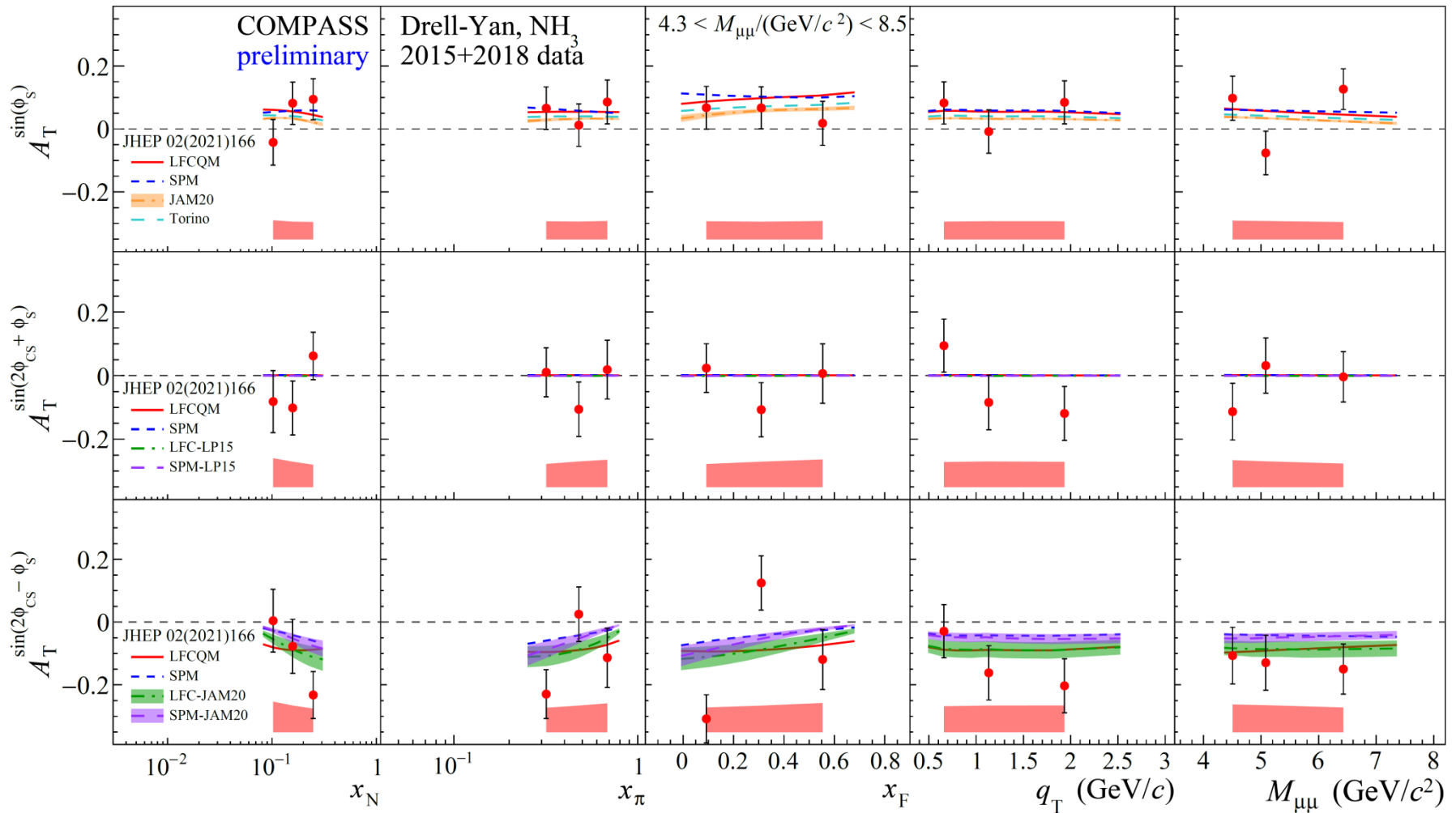
$$\frac{d\sigma^{LO}}{dq^4 d\Omega} \propto F_U^1 \left(1 + \cos^2 \theta_{CS}\right) \left\{ 1 + \dots \right. \\ \left. + S_T \begin{bmatrix} A_T^{\sin \varphi_S} \sin \varphi_S \\ + D_{[\sin^2 \theta_{CS}]} \left(A_T^{\sin(2\varphi_{CS} - \varphi_S)} \sin(2\varphi_{CS} - \varphi_S) \right. \\ \left. + A_T^{\sin(2\varphi_{CS} + \varphi_S)} \sin(2\varphi_{CS} + \varphi_S) \right) \\ + D_{[\sin 2\theta_{CS}]} \left(A_T^{\sin(\varphi_{CS} - \varphi_S)} \sin(\varphi_{CS} - \varphi_S) \right. \\ \left. + A_T^{\sin(\varphi_{CS} + \varphi_S)} \sin(\varphi_{CS} + \varphi_S) \right) \end{bmatrix} \right\}$$

COMPASS 2015 + 2018 NEW!



DY TSAs at COMPASS (high-mass range)

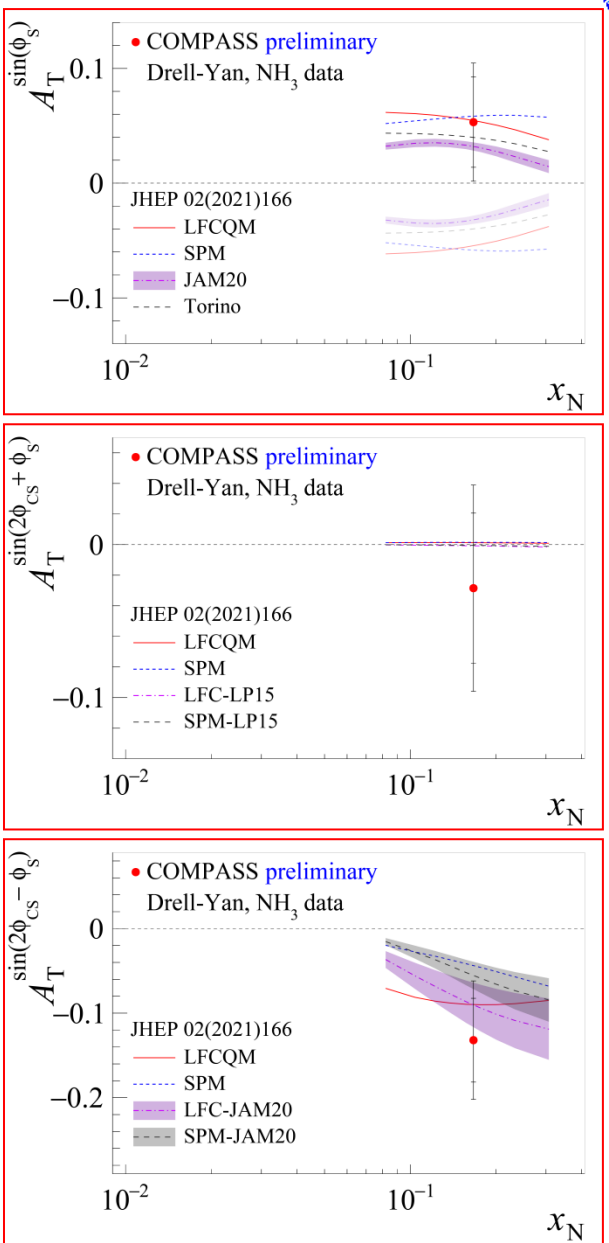
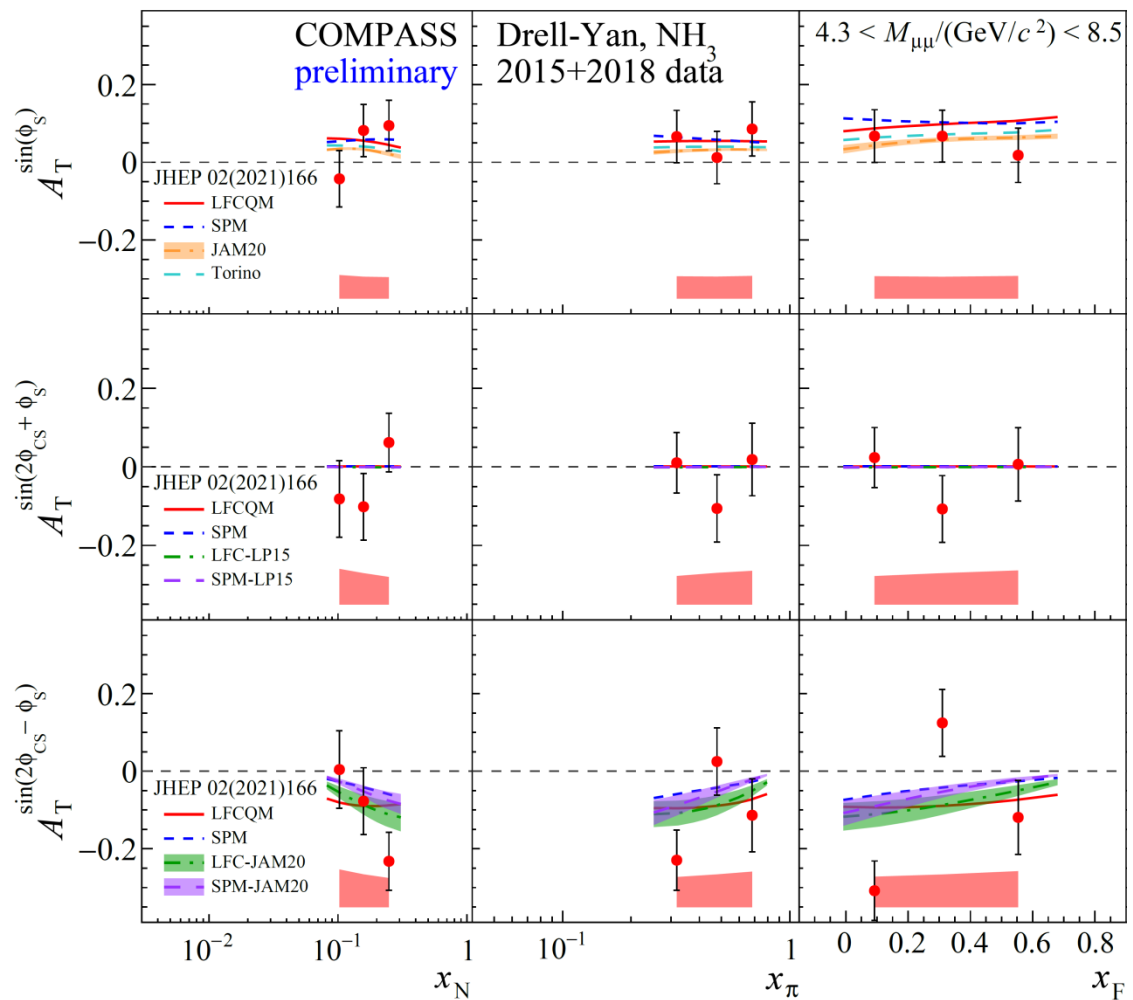
Theory curves based on S. Bastami et al. JHEP 02, (2021),166



- General agreement with available theory predictions

DY TSAs at COMPASS (high-mass range)

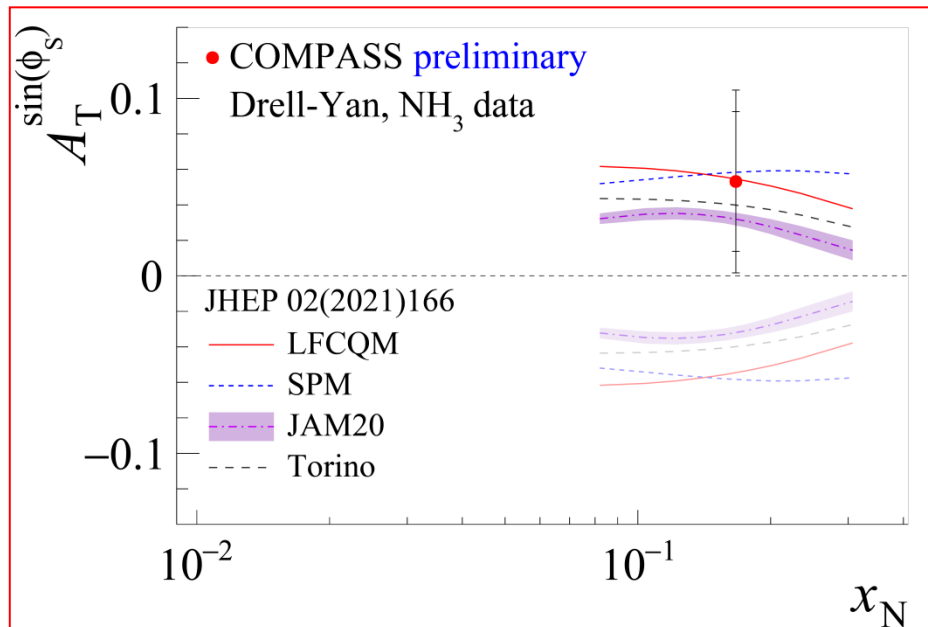
Theory curves based on S. Bastami et al. JHEP 02, (2021),166



- General agreement with available theory predictions

Conclusions

- During phase I COMPASS has measured all possible SIDIS TSAs.
 - Non-zero Sivers and Collins SIDIS-TSAs in the Drell-Yan “high-mass range”:
PLB 770 (2017) 138
- In 2017 COMPASS has published the results for the **first polarized DY measurements**: PRL 119, 112002 (2017)
- The second year of polarized DY data-taking was performed in 2018
- Re-production and re-analysis of both 2015 2018 data is over
- Final results have been presented today:
the paper is in preparation
- **COMPASS data favors the sign-change of Sivers TMD PDF**



STAR WARS DAY™
MAY THE 4TH
BE WITH YOU